Check for updates

Molecular Ecology

WILEY

MOLECULAR ECOLOGY

ORIGINAL ARTICLE OPEN ACCESS

Phylogeographic Breaks With and Without Contemporary Barriers to Migration in the Lizard *Acanthodactylus erythrurus*

Filipe Gomes de Almeida[1,2] | Loïs Rancilhac[1,3,4] | Laure Benoit[5] | Anne Loiseau[5] | Menad Beddek[1] | Abdellah Bouazza[6] | José Carlos Brito[7,8,9] | Laghzaoui El-Mustapha[10] | Aurélien Miralles[1,11] | Philippe Geniez[12] | Raphaël Leblois[5] | Pierre-André Crochet[1]

[1]CEFE, CNRS, Univ Montpellier, EPHE, IRD, Montpellier, France | [2]Department of Physical Geography and Ecosystem Science, Lund University, Lund, Sweden | [3]Animal Ecology, Department of Ecology and Genetics, Evolutionary Biology Centre, Uppsala University, Uppsala, Sweden | [4]Department of Biodiversity and Evolutionary Biology, National Museum of Natural Sciences, Spanish National Research Council (CSIC), Madrid, Spain | [5]CBGP, INRAE, CIRAD, IRD, Institut Agro, Univ Montpellier, Montpellier, France | [6]Laboratoire Génie Géo-Bio-Environnement et Innovation, FP Taroudant, Université Ibn Zohr, Agadir, Morocco | [7]CIBIO, Centro de Investigação Em Biodiversidade e Recursos Genéticos, InBIO Laboratório Associado, Campus de Vairão, Universidade Do Porto, Vairão, Portugal | [8]BIOPOLIS Program in Genomics, Biodiversity and Land Planning, CIBIO, Vairão, Portugal | [9]Department of Biology, Faculty of Sciences, University of Porto, Porto, Portugal | [10]ISPITS - Higher Institute of Nursing Professions and Health Techniques of Marrakech, Kenitra, Morocco | [11]Institut de Systématique, Évolution, Biodiversité (ISYEB), Muséum national d'Histoire naturelle, CNRS, Sorbonne Université, EPHE, Université Des Antilles, Paris cedex, France | [12]CEFE, EPHE-PSL, Univ Montpellier, CNRS, Biogéographie et Ecologie des Vertébrés, Montpellier, France

Correspondence: Loïs Rancilhac (loisrancilhac@gmail.com)

Received: 2 October 2025 | **Revised:** 22 April 2026 | **Accepted:** 28 April 2026

Keywords: environmental gradients | hybrid zones | phylogeographic breaks | reptiles | speciation

ABSTRACT

Identifying phylogeographic breaks and deciphering the relative contributions of environmental extrinsic (e.g., geological barriers, ecological gradients) and organismal intrinsic (e.g., limited dispersal, reproductive incompatibilities) factors to their persistence remain challenging, especially in the absence of genomic data. Here, we address this issue using parapatric lineages of the lizard *Acanthodactylus erythrurus* in south-western Morocco. A previous study based on nine nuclear loci identified two phylogeographic units (coastal vs. inland) whose separation did not align with landscape features preventing migration. The coastal lineage was inferred to evolve under isolation by distance (IBD, the regular increase of genetic differentiation with geographic distance), despite the presence of large rivers across its range. This suggests either that phylogeographic breaks do not align with landscape features, or that the restricted marker set prevented an accurate inference of phylogeographic breaks. We tested these hypotheses using RADseq data and recovered three lineages, each separated by phylogeographic breaks and narrow contact zones with restricted admixture. Coastal populations that had been previously identified to evolve under IBD actually included two lineages separated by a major, permanent river, reducing migration. The inland phylogeographic break, correctly identified by the previous study, is located in a continuously distributed habitat. Neither of the breaks aligned with steep changes in bioclimatic variables, suggesting a negligible contribution of local adaptation. We conclude that intrinsic reproductive barriers, as evidenced by narrow clines in allele frequencies at multiple loci spread over the genome, play a major role in maintaining these phylogeographic breaks. Our results also highlight the difficulty of identifying phylogeographic breaks from pre-genomic molecular data.

Filipe Gomes de Almeida and Loïs Rancilhac equal contributions.

This is an open access article under the terms of the Creative Commons Attribution-NonCommercial-NoDerivs License, which permits use and distribution in any medium, provided the original work is properly cited, the use is non-commercial and no modifications or adaptations are made.

© 2026 The Author(s). *Molecular Ecology* published by John Wiley & Sons Ltd.

1 | Introduction

Phylogeographic breaks—discontinuities in the geographic distribution of genetic diversity—are an outstanding phylogeographic pattern that can provide valuable information about historical and contemporary isolation of populations (Avise 2000). They typically form when populations isolated by geographical barriers to gene flow accumulate genetic divergence with time in allopatry (Kuo and Avise 2005). These vicariance episodes constitute the main engine of biodiversity, as the vast majority of independent evolutionary units are believed to originate from a phase of geographical isolation (Coyne and Orr 2004). Such allopatric divergence may lead to speciation (i.e., the evolution of reproductive isolation across evolutionary lineages; Stankowski and Ravinet 2021) through the accumulation of genetic incompatibilities, or local adaptation to divergent environments. Yet, not all vicariance events lead to speciation: if the time spent in allopatry is too short for reproductive barriers to evolve, lineages may merge upon secondary contact (Garrick et al. 2019). One of the main aims of phylogeography is to understand the relative contributions of speciation and geographical barriers to gene flow in maintaining contemporary spatial genetic diversity. Therefore, the factors underlying the separation of phylogeographic lineages must be carefully investigated to determine whether they are reproductively isolated, separated by geographical barriers to gene flow, or represent the legacy of past vicariance that is gradually homogenizing following secondary contact.

In many cases, phylogeographic breaks coincide with contemporary barriers to migration (i.e., breaks in population connectivity; e.g., Leaché et al. 2020). However, barriers to migration can disappear with time, allowing for secondary contact of genetically differentiated lineages. In that case, the persistence of genetic differentiation will depend on intrinsic reproductive barriers, as well as ecological differentiation and small-scale spatial segregation. Considering that the build-up of intrinsic reproductive barriers in allopatry is a long process, it is possible that time in isolation is the main driver of phylogeographic breaks in the absence of extrinsic barriers to gene flow. By comparison, local adaptation may disproportionately contribute to phylogeographic structure at small time scales because adaptation to divergent environments can lead to a rapid evolution of extrinsic reproductive isolation (Schluter 2009). Steep ecological transitions may contribute to maintaining divergence by enforcing pre-zygotic isolation when the spatial or temporal distributions of divergent lineages differ (e.g., in cases of phenological differences or small-scale spatial segregation by habitat, Grossenbacher et al. 2014; Taylor and Friesen 2017), or extrinsic post-zygotic isolation when hybrids are maladapted to environmental conditions (Coyne and Orr 2004). The interplay of these factors within and across species and geographic areas is not well understood. If extrinsic factors such as geographical barriers to migration or local adaptation play a major role in phylogeographic structuring, we expect that phylogeographic breaks coincide with existing barriers or steep environmental changes. On the other hand, the location of phylogeographic breaks maintained by intrinsic reproductive barriers would be determined by past demographic dynamics, population densities and landscape resistance to dispersal (Barton and Hewitt 1985). Studying the geographic distribution of phylogeographic breaks and their concordance with geological and ecological features can yield valuable insight into the processes maintaining genetic diversity at the landscape level.

Another difficulty is that the accurate detection of phylogeographic breaks is not a straightforward endeavour, as spurious signals of discontinuity can be detected in continuous populations (e.g., evolving under isolation by distance [IBD]), especially in the presence of large sampling gaps (Audzijonyte and Vrijenhoek 2010; Irwin 2002; Kuo and Avise 2005; Tolley et al. 2022). Conversely, phylogeographic breaks may be under-detected when the molecular markers used are not informative enough (Doniol-Valcroze et al. 2024). Mitochondrial DNA (mtDNA) has long been the marker of choice to investigate geographical patterns of genetic diversity, but phylogeographic breaks in mtDNA do not necessarily align with those in nuclear markers (Dufresnes, Nicieza, et al. 2020; Toews and Brelsford 2012; Zhang et al. 2019). However, developments of sequencing technologies now allow the collection of thousands of nuclear markers even in non-model organisms. Analysing phylogeographic patterns in a diversity of organisms based on genome-wide genotypes, through thorough spatially explicit statistical frameworks, is crucial to further our understanding of the factors underlying the maintenance of phylogeographic breaks across the tree of life.

Such approaches are especially needed in regions and taxonomic groups where the inventory of biodiversity is still incomplete. These biodiversity knowledge shortfalls hinder conservation planning (Carné and Vieites 2024), and also bias our understanding of speciation (e.g., the timing of speciation or spatial scale of speciation processes; Stankowski et al. 2024; Struck et al. 2018) or biodiversity patterns (e.g., levels of endemisms and ecological specialization, Hortal et al. 2015). Such shortfalls are not uniformly distributed over the globe; even in relatively well studied areas such as the Mediterranean Basin, the amount of data available to address biodiversity shortfalls varies drastically between regions. This is especially notable between the northern and southern sides of the Mediterranean sea (Perret et al. 2023) and several areas where biodiversity is still likely underestimated have been identified, including for reptiles (Ficetola et al. 2013).

The Fringe-fingered lizard *Acanthodactylus erythrurus* species complex is widespread in the Iberian Peninsula and the Maghreb (the north-western part of North Africa from Morocco to Libya). Recent studies using mitochondrial DNA (mtDNA) and multi-locus nuclear markers have uncovered a high level of genetic diversity and complex phylogeographic structure (Fonseca et al. 2009; Harris et al. 2024; Rancilhac et al. 2023) with many deep lineages, some of which represent valid species (Doniol-Valcroze et al. 2024; Miralles et al. 2020). The situation in Morocco is particularly fascinating, as the country harbours at least 11 mitochondrial lineages (Figure 1) whose initial diversification was estimated around 10 Ma ago (Miralles et al. 2020; Rancilhac et al. 2023). However, using nine nuclear markers, Rancilhac et al. (2023) recovered a much weaker genetic structuring. Using a spatially explicit framework, these authors concluded that all Moroccan populations could be divided into at least four vicariant lineages, within which populations were hypothesized to evolve under

13652294x, 2026, 19, Downloaded from https://onlinelibrary.wiley.com/doi/10.1111/mec.70555 by Uppsala University Library, Wiley Online Library on [20/10/2026]. See the Terms and Conditions (https://onlinelibrary.wiley.com/terms-and-conditions) on Wiley Online Library for rules of use; OA articles are governed by the applicable Creative Commons License

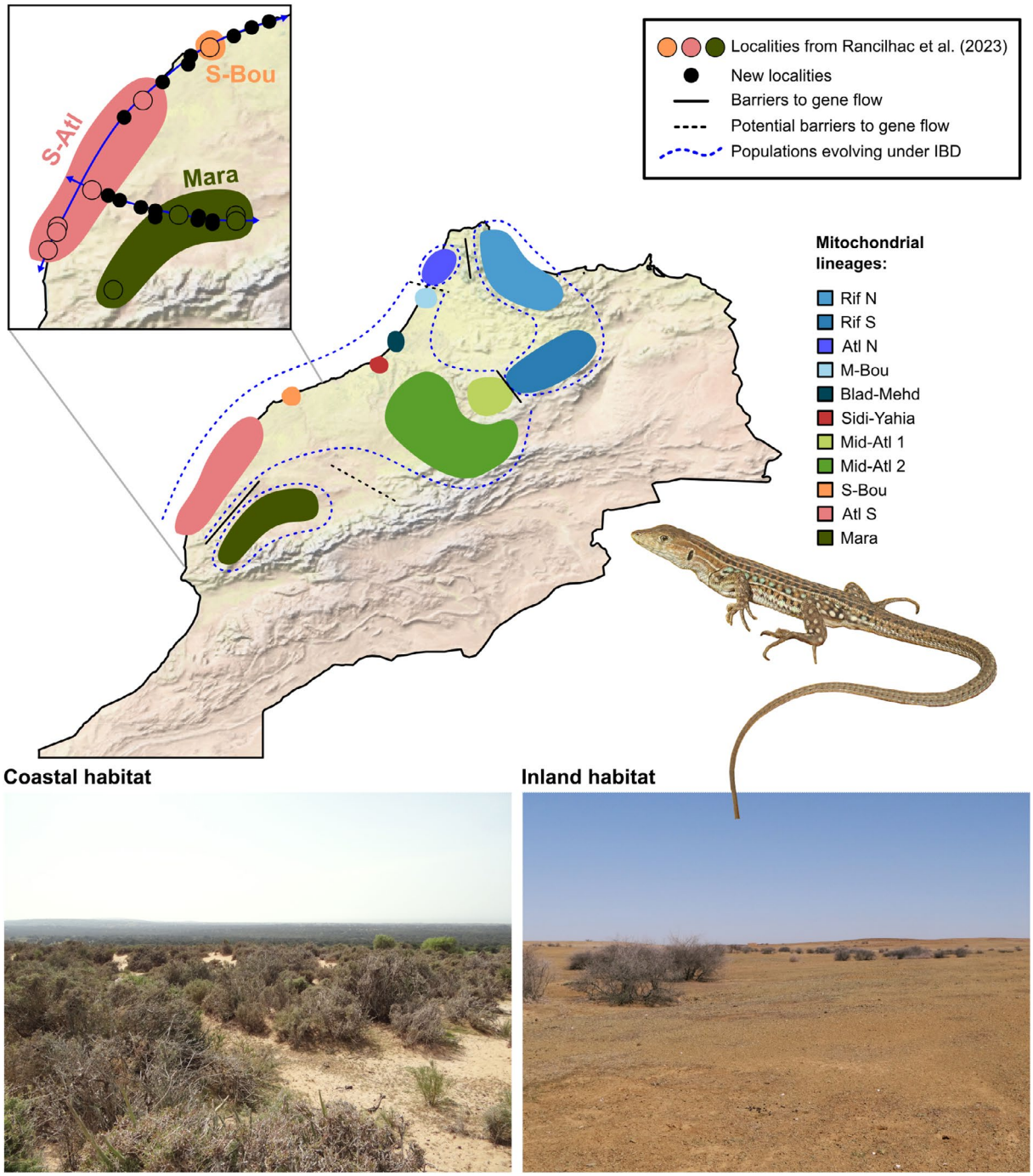

FIGURE 1 | Summary of the phylogeography of *Acanthodactylus erythrurus* in Morocco. Coloured shapes show the distribution of the 11 mitochondrial lineages identified by Miralles et al. (2020) and Rancilhac et al. (2023). Dotted blue lines show groups of populations evolving under isolation by distance while straight black lines show barriers to gene flow (solid: Strongly supported, dotted: Requiring further investigation) as suggested by nuclear markers (Rancilhac et al. 2023; Doniol-Valcroze et al. 2024). The inset shows the study area of the present study, with coloured dots illustrating localities sampled by Rancilhac et al. 2023 and black dots new localities sampled for this study. The two blue arrows show the transects used for geographic cline analyses. Modified from Rancilhac et al. 2023. The photos illustrate an *A. erythrurus* specimen from the S-Atl lineage (Wouter Beukema, used with permissions), and examples of coastal (left, Essaouira region, P.-A.C.) and inland habitats (right, Oued Tensift valley, P.-A.C.).

IBD, suggesting that mtDNA largely overestimated the number of phylogeographic breaks. However, analyses of a subset of these populations in north-eastern Morocco (Rif and Middle-Atlas mountain ranges) based on genome-wide data demonstrated that increasing the number of markers improved the identification of phylogeographic breaks as some populations where IBD could not be excluded with the nine nuclear markers represented in fact two vicariant species-level lineages (Doniol-Valcroze et al. 2024). The situation is even more puzzling along the Atlantic coast of Morocco where six mtDNA lineages occur, but only one phylogeographic break could be detected from the nuclear data, near Larache in Northern Morocco (Rancilhac et al. 2023). This result is surprising, as several large rivers exist along the coast that

1365294x, 2026, 19, Downloaded from https://onlinelibrary.wiley.com/doi/10.1111/mec.70555 by Uppsala University Library, Wiley Online Library on [20/10/2026]. See the Terms and Conditions (https://onlinelibrary.wiley.com/terms-and-conditions) on Wiley Online Library for rules of use; OA articles are governed by the applicable Creative Commons License

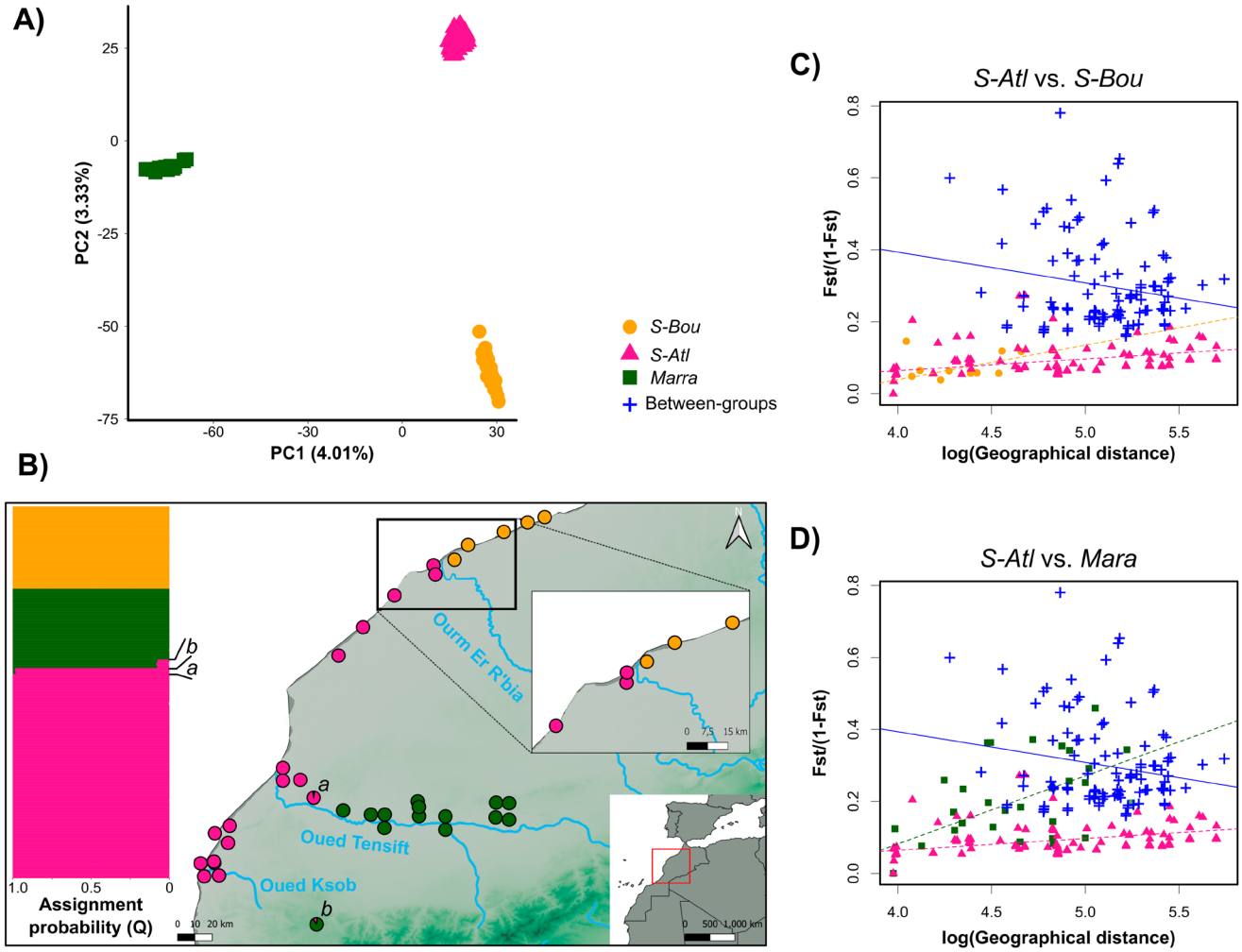

FIGURE 2 | Results of population structure analyses. (A) Principal Component Analysis (PCA) scatterplot of 19,188 unliked SNPs. (B) Results of STRUCTURE clustering with three groups (best clustering solution). Left: Barplot showing individual assignment probabilities to the three groups (each bar is a single individual); Right: Map of the study area with assignment probabilities shown as pie charts for each sampling locality. a and b indicate two localities where small levels of admixture between Mara and S-Atl were identified. (C) Regressions of genetic against geographic distances within S-Atl and S-Bou (triangles and circles) and between them (crosses). (D) Regressions of genetic against geographic distances within S-Atl and Mara (triangles and squares) and between them (crosses). In C and D, dotted and solid lines show within-group and between-groups regressions, respectively.

could act as strong barriers to migration (Figure 2b), although this effect is not universal in lizards (Fonseca et al. 2024; Gonçalves-Sousa et al. 2022; Peixoto et al. 2020; Pounds and Jackson 1981). We propose three non-exclusive hypotheses to explain this result: (1) the poor resolution of the markers used by Rancilhac et al. (2023) resulted in an underestimation of the number of phylogeographic breaks along the Atlantic coast; (2) rivers are not efficient barriers to dispersal in *A. erythrurus*; or (3) contemporary barriers to dispersal do not correlate with phylogeographic breaks.

To test these hypotheses, we used a Restriction Site-Associated DNA sequencing (RADseq) protocol to generate thousands of genome-wide Single Nucleotide Polymorphisms (SNPs) from coastal and inland *A. erythrurus* populations in South-Western Morocco. We also substantially enriched our sampling along two new transects connecting three previously identified mitochondrial lineages, and then reconstructed the phylogeographic history of these populations. Our aims are as follows: (1) verify if the findings of previous studies based on a few markers, specifically the presence of a phylogeographic break between inland (*Mara*) and coastal (*S-Atl*) populations but absence of break along the Atlantic coast, still hold when evaluated with genomic data; (2) assess levels of reproductive isolation between lineages in contact zones to get insights into the role of speciation in maintaining these lineages; and (3) assess whether phylogeographic breaks are associated with contemporary geographic features and ecological transitions.

2 | Material and Methods

2.1 | Design and Sampling

Our sampling focuses on three of the previously described *A. erythrurus* mtDNA lineages (figure 1; terminology of lineages follows Rancilhac et al. 2023): *Mara* (inland plains surrounding Marrakech), *S-Atl* (Southern Atlantic coast from Ouled Ghanem

1365294x, 2026, 19, Downloaded from https://onlinelibrary.wiley.com/doi/10.1111/mec.70555 by Uppsala University Library, Wiley Online Library on [20/10/2026]. See the Terms and Conditions (https://onlinelibrary.wiley.com/terms-and-conditions) on Wiley Online Library for rules of use; OA articles are governed by the applicable Creative Commons License

to Essaouira) and *S-Bou* (single locality of Sidi-Boumaine, south of Casablanca). Analyses by Rancilhac et al. (2023) suggested that *Mara* is separated from the neighbouring coastal populations by a phylogeographic break, although no clear geographic barrier to migration exists. On the other hand, the divergence between *S-Atl* and *S-Bou* was found to be compatible with a single IBD gradient, although several rivers exist between them (e.g., Oued Tensift within *S-Atl*, Oum Errabia between *S-Atl* and *S-Bou*).

Our samples include 131 *A. erythrurus* individuals collected during field trips in 2004–2019, in and around the previously identified ranges of *Mara, S-Atl* and *S-Bou* (Figure 1, Table S3). This sampling covers the localities included in Rancilhac et al. (2023), as well as new localities. Additional sampling (13 localities, 49 samples) was specifically designed to cover two geographic transects: first along the Atlantic coast through *S-Atl* and *S-Bou* northwards almost to Casablanca; secondly from the most inland *Mara* localities to the closest coastal populations (Figure 1). To infer the time frame of the divergence of *Mara*, *S-Atl* and *S-Bou*, we produced a time-calibrated phylogeny by adding 46 additional *Acanthodactylus* samples from Tunisia, Algeria, Morocco and Spain: five samples of most *A. erythrurus* mtDNA lineages described in Rancilhac et al. (2023) (except for Central Algeria with only three samples) and three of the outgroup *Acanthodactylus savignyi*. The complete list of samples used is provided in Table S1.

2.2 | RADseq Library Preparation and Sequencing

We used the Restriction-site Associated DNA sequencing (RADseq) protocol described in Doniol-Valcroze et al. (2024) to produce reduced representations of the genomes of our samples. Total genomic DNA was extracted using the 96-Well Animal Genomic DNA Miniprep Kit (Biobasic) following the manufacturer's recommended procedures. RADseq libraries were prepared by digesting 180 ng of genomic DNA from each sample with the enzyme *SbfI*. P1 adapters (synthesized by IDT, USA) and barcodes (Multiplex IDentifiers: MIDs) were then ligated to the digested fragments. To increase diversity within the library and reduce the number of phasing errors, a set of 32 MIDs of 6 and 7 base pairs (bp) was used. Final enrichment PCR amplification was performed in 3 independent 25 μL wells with an initial amount of 30 ng of DNA and 14 PCR cycles. PCR products were pooled and homogenized, and the obtained library was quantified by qPCR using the Library Quantification Kit-Illumina/Universal (KAPA; KK4824) for sequencing preparation. The library was then denatured using NaOH and diluted to 7 pM prior to clustering. Clustering and 100 bp pair-end read sequencing were performed on two lanes of a NovaSeq 6000 flowcell at MGW (Montpellier GenomiX) following the manufacturer's instructions. A low-concentration spike-in (1%) of PhiX Control v3 was used as an in-lane positive control for alignment calculations and quantification efficiency.

2.3 | Bioinformatic Processing of the Data

We demultiplexed and trimmed raw reads to 90 bp using *process_radtags* in Stacks v2.2 (Rochette et al. 2019) and Trimmomatic v0.39 (Bolger et al. 2014). We performed *de novo* assembly of RAD loci for two separate sample sets: Assembly 1 included the samples from *Mara, S-Atl* and *S-Bou* exclusively, while Assembly 2 included the expanded sampling for phylogenetic inferences. We removed PCR duplicates with Stacks *clone_filter*, after which we ran the complete Stacks *de novo* pipeline (i.e., *ustacks, cstacks, sstacks, tsv2bam, gstacks*). We followed the '80% rule' introduced by Paris et al. (2017) to optimize the minimal read depth to form clusters and the number of mismatches allowed between stacks to merge them into a locus (parameters *m* and *M* in *ustacks*), as well as the number of mismatches allowed to cluster loci (parameter *n* in *cstacks*). This approach consists in selecting parameters that optimize the number of polymorphic loci shared by 80% of the samples. We used an incremental approach, first assembling loci with *m* ranging 3–7 and default values for *M* and *n*. We selected an optimal value for *m*, and subsequently assembled loci with *M* ranging 1–8 and *n* left to default. Finally, we tested *n* values corresponding to $M-1$, M and $M+1$. We used the RADStackhelpR (DeRaad 2021) and vcfR (Knaus and Grünwald 2017) packages in R v4.2.3 (R Core Team 2023) to calculate summary statistics from Stacks VCF outputs, visualize assembly statistics and determine the best parameter values.

2.4 | Population Structure Analyses

We investigated population structure across the *Mara, S-Atl*, and *S-Bou* localities by performing a Principal Component Analysis (PCA) based on the SNPs from Assembly 1. We first used Stacks *populations* to randomly select one SNP per locus and filter out all sites with missing genotypes and ran a preliminary PCA using the R package ade4 v1.7–22. Next, to maximize the amount of SNPs included in the analysis, we allowed sites with $\leq 5\%$ missing genotypes and imputed the missing genotypes in each lineage separately with the random forest algorithm implemented in the missForest v1.5 R package (Stekhoven and Bühlmann 2012) with default settings. The final PCA analyses were done with the imputed dataset (see also Text S1).

Next, we jointly inferred population structure and individual ancestries with the Bayesian clustering algorithm STRUCTURE v2.3.4 (Pritchard et al. 2000) using the complete imputed SNP set. We repeated the analysis with numbers of groups (K) ranging from 1 to 6 and four replicates each. We used the admixture model, set the POPALPHAS parameter to TRUE (POPALPHAS = 1, allowing separate α for each population where α is the ancestry prior, see Pritchard et al. 2010; Wang 2017; Toyama et al. 2020), set up MCMC chains with 10,000 burn-in steps followed by 100,000 iterations, and left the remaining settings as default. We selected the best-fitting K value as that maximizing the incremental increase in likelihood, DeltaK, using the method developed by Evanno et al. (2005) and implemented in STRUCTURE HARVESTER (Earl and vonHoldt 2012). For the best K value, we merged individual assignment probabilities (Q) from the four runs with CLUMPP (Jakobsson and Rosenberg 2007). Finer-scale examination of population structure and within lineages genetic diversity can be found in Text S1 and Figures S4–S7.

13652394x, 2026, 19, Downloaded from https://onlinelibrary.wiley.com/doi/10.1111/mec.70555 by Uppsala University Library, Wiley Online Library on [20/10/2026]. See the Terms and Conditions (https://onlinelibrary.wiley.com/terms-and-conditions) on Wiley Online Library for rules of use; OA articles are governed by the applicable Creative Commons License

2.5 | Test of Phylogeographic Breaks

To verify whether the partition into three groups indicated the presence of phylogeographic breaks, as opposed to IBD, we used statistical tests based on linear regressions of genetic against geographic distances within and between lineages (Hausdorf and Hennig 2020). In brief, assuming two groups of populations with similar within-group regressions, one can statistically test whether a regression on between-group distances differs from a regression on pooled within-group distances using a non-parametric jackknife test. If this is the case, then the data support a phylogeographic break separating the two groups. More details on this test can be found in Hausdorf and Hennig (2020).

We applied this approach to the two pairs of geographically adjacent groups: *Mara* v. *S-Atl* and *S-Atl* v. *S-Bou*. For each pair of sampling localities, we estimated F_{st} using Stacks *population* (filters applied: -R 0.95, --write-ramdom-snp, --fstats, --genepop). Geographic distances between each pair of populations were estimated from their geographic coordinates using the prabclus v2.3-3 package (Hausdorf and Hennig 2020). When a locality was represented by a single sample, we lumped it with its closest neighbour. We then fitted linear regression between $\frac{F_{st}}{1-F_{st}}$ and log-transformed geographic distances, and compared the within-group and between-group regressions using prabclus.

2.6 | Geographic Cline Analyses

Having confirmed the presence of phylogeographic breaks due to past vicariance across the three groups (cf. results for details), we used geographic cline analyses across two transects to investigate geographic patterns of introgression and the levels of reproductive isolation across lineages (Barton 1979; Dufresnes, Pribille, et al. 2020; Szymura and Barton 1986). The *S-Atl* to *Mara* transects runs from the mouth of the Oued Tensift river on the Atlantic coast (near Souira-Plage) inland along the valley of the Oued Tensift to the north of Marrakech (Figures 1 and 2B). No major topographical barriers exist, but the area has been extensively modified by the recent expansion of agriculture and *A. erythrurus* populations are now fragmented in remnant patches of uncultivated steppes with thorny bushes or riverines sandbeds. The *Sbou* to *S-Atl* transect runs along the Atlantic coast where suitable sandy dune habitats remain fairly continuous, but where several large rivers cut the coastline. Both transects and their respective habitats are visible on the satellite image layer provided as Data S1.

For each transect, we calculated the distance from each population and one of the distal localities arbitrarily defined as the start, using Haversine's formula implemented in the geosphere v1.5-18 R package. We first fitted sigmoid clines to changes in Structure's Q values along the transects. We ran STRUCTURE separately for each transect including only the relevant localities and with a fixed $K=2$. We set the remaining parameters as before. We then used Hzar v0.2–5 (Derryberry et al. 2014) to fit sigmoid clines to the Q values along the two transects. We tested four cline models differing by the presence or absence of exponential introgression tails (none, on both sides or only one side), with minimum and maximum Q values estimated from the data. We also tested a null model where ancestries do not change along the transects, and selected the best fitting model for each transect using the Akaike information criterion (AIC). Secondly, we repeated this analysis using allele frequencies at diagnostic SNPs (i.e., SNPs that were differentially fixed in allopatric populations). To avoid misidentification of diagnostic SNPs due to genotyping errors, we used the two most distal populations of each lineage to estimate differences in allele frequencies. For each transect, we used Stacks *Populations* to extract a single SNP per locus and retain sites with ≤20% missing genotypes and at least one sample per locality. We recovered 734 diagnostic SNPs for the *Mara* to *S-Atl* transect, and 220 for *S-Atl* to *S-Bou*. Allele frequencies at each locality were estimated using the *population* module in Stacks (--hzar flag) and individual clines were fitted to each SNP with model selection as described above.

2.7 | Variation of Environmental Variables Along the Transects

We investigated whether contact zones coincided with steep environmental gradients by quantifying the changes in several climatic variables along the two transects. We downloaded data from the remote-sensing WorldClim dataset (Fick and Hijmans 2017) at a resolution of 30 s and extracted measures of the 19 BioClim variables at each sampling point along the two transects with the terra v1.7.23 R package. For each transect separately, we used a PCA to summarize variation in environmental variables and used the scores at the Principal Components (PCs) explaining most of the environmental variance to investigate whether the genomic clines coincided with sharp ecological transitions (Ruegg 2008). Finally, we tested whether ecological distance between localities could explain genetic differentiation while accounting for geographic distance, using a isolation by environment framework, as detailed in Text S2.

2.8 | Phylogenetic Reconstruction and Divergence Time Estimate

Our population genetics analyses consistently supported that *Mara, S-Atl* and *S-Bou* formed three well differentiated genetic groups. In order to complement our understanding of their phylogeographic history, we inferred a timetree including most mitochondrial lineages within the *A. erythrurus* complex. We produced four concatenation matrices from Assembly 2, retaining loci with ≤60%, 40%, 20% or 10% of missing samples. We output the concatenation of the retained loci (including variant and invariant sites) in phylip format, with heterozygous positions encoded as IUPAC uncertainty characters (--phylip-var-all flag in *populations*). We then ran a first round of phylogenetic analyses that had two goals: (1) ensuring that filtering strategies did not impact the reconstructed relationships, and (2) verifying that the Iberian populations are sister to the closest Moroccan populations (Rif lineage), which would enable us to use the end of the Messinian salinity crisis as a calibration point (Rancilhac et al. 2023). This is the most recent time at which Morocco and the Iberian Peninsula were connected by a land bridge 5.4 million years ago (mya; Krijgsman et al. 1999). We performed maximum likelihood (ML) phylogenetic inferences with IQTREE v1.6.8 (Nguyen et al. 2015), estimated the best substitution

13652394x, 2026, 19, Downloaded from https://onlinelibrary.wiley.com/doi/10.1111/mec.70555 by Uppsala University Library, Wiley Online Library on [20/10/2026]. See the Terms and Conditions (https://onlinelibrary.wiley.com/terms-and-conditions) on Wiley Online Library for rules of use; OA articles are governed by the applicable Creative Commons License

model with ModelFinder (Kalyaanamoorthy et al. 2017) and branch support with the inbuilt Shimodaira-Hasegawa-like (SH) approximate likelihood test (aLRT; Guindon et al. 2010) with 1000 pseudoreplicates.

The filtering strategy had no impact on the recovered topology, and the Iberian and Rif lineages were always recovered as sisters with full support. Next, we calibrated the inferred phylogenies using the Least-Square Dating method implemented in IQTREE v2.2.6 (LSD; To et al. 2016). Because the amount of missing data in the data matrices can strongly impact branch length in downstream phylogenetic analyses, and thus split time estimates, we calibrated the phylogenies obtained from matrices with permitted levels of missing data ranging from 10% to 60%. We constrained the divergence between the Iberian and Rif lineages to 5.4 mya and estimated confidence intervals around the split times with the --date-ci option and 100 resamplings of branch lengths.

3 | Results

3.1 | RADseq Data Assembly

The sequencing of the RADseq libraries yielded 1,719,963,194 raw read pairs, of which 613,491,320 were retained after quality filtering and PCR duplicates removal. Rates of PCR duplicates were high, with an average of 63.08% ± 3.82% (SD) of the reads removed. We performed *de novo* assembly of the reads into loci using the following parameters: $m = 3$, $M = 4$, and $n = 5$, which maximized the number of loci shared by > 80% of the samples in both assemblies (Figures S1 and S2). Assembly 1, restricted to the *Mara, S-Atl* and *S-Bou* lineages, yielded 19,209–36,561 loci (19,188–36,561 unlinked SNPs), depending on populations included (Table 1). After filtering, average depths of coverage per individual ranged from 4.9 to 83.1 X (mean 32.05 ± SD 13.29 X). Assembly 2, including representatives from the whole *A. erythrurus* complex, included 17,374–51,088 RAD loci (701,532–3,389,274 SNPs), depending on the levels of missing data allowed.

TABLE 1 | Summary statistics of the RADseq assemblies: Number of loci and SNPs recovered for each assembly and downstream filterings.

Assembly	Number of Loci	Number of SNPs
Assembly 1 (population genetics)		
All localities	19,209	19,188
S-Atl to *Mara* transect	34,070	33,994
S-Bou to *S-Atl* transect	36,580	36,561
Assembly 2 (phylogeny)		
60% missing data	51,088	3,389,274
40% missing data	40,720	2,501,067
20% missing data	28,397	1,455,835
10% missing data	17,374	701,532

Note: Assembly 1 included 131 samples from South-western Morocco only, while assembly 2 included 177 samples from the whole *Acanthodactylus erythrurus* complex.

3.2 | Population Structure

A PCA based on 19,188 unlinked SNPs from Assembly 1 delineated three distinct clusters (Figure 2A), without clear intermediate samples: *Mara*, which occurs inland starting 28 km from the Atlantic coast; *S-Atl*, which inhabits a~15 km wide coastal strip, reaching the Oum Er R'bia river in the north; and *S-Bou*, expanded from the analyses of Rancilhac et al. (2023) to include all coastal localities north of the Oum Er R'bia river to Casablanca. STRUCTURE supported an optimal clustering solution with three groups, perfectly matching the PCA clusters (Figure 2B, Figure S3). The four replicates were highly consistent, with low variance in posterior probability (mean log likelihood of the data −344580.50 ± SD 23.46). Again, signals of admixture were very weak, with most samples having assignment probabilities (Q) > 0.98 (detailed assignment probabilities per individual are given in Table S3), including in neighbouring localities of different groups. Interestingly, the only *S-Atl* population with traces of admixture (although minimal: Q≈0.08, Table S3) is the closest one to *Mara* along the transect (population 'a' in Figure 2B). Yet, the clearest signal of admixture came from an isolated locality in the southern edge of *Mara*'s range but far from any sampled population of *S-Atl*, where the three sampled individuals had a Q = 0.92 for *Mara* and Q = 0.08 for *S-Atl*.

Distance between the closest populations of each lineage varied between the two transects. In the *S-Atl* to *Mara* transect, a 19 km gap separates the easternmost *S-Atl* samples from the westernmost *Mara* samples. Suitable habitats in this gap are scarce, small and isolated (P.-A.C., pers. obs.) and attempts to find lizards in this area failed. In the *Sbou* to *S-Atl* transect, less than 1 km separates the two lineages, with populations of each sampled on opposite sides of the Oum Er′bia river mouth.

3.3 | Isolation by Distance Tests

In all three groups, we found a positive correlation between genetic and geographic distances ($R^2 = 0.34$, 0.13 and 0.34; slopes = 0.10, 0.03 and 0.19 for *S-Bou*, *S-Atl* and *Mara*, respectively; Figure S8). Within-group regressions in the three groups were statistically similar ($p = 1.0$ for *S-Atl* vs. *S-Bou*, and $p = 0.14$ for *S-Atl* vs. *Mara*), allowing us to pool within-group distances and compare them to between-group distances. In both comparisons, regressions based on within- and between-group distances differed significantly ($p = 0.038$ for *S-Atl* vs. *S-Bou*, and $p = 1.24e^{-6}$ for *S-Atl* vs. *Mara;* Figure 2C,D), with the latter showing negative slopes. This result confirms that neighbouring lineages are separated by phylogeographic breaks.

3.4 | Geographic Cline Analyses

Q values along the S-Atl—Mara transect were best modelled by a simple sigmoid cline without introgression tails (Figure 3A), with an estimated width of 0.61 km, although with substantial

13652394x, 2026, 19, Downloaded from https://onlinelibrary.wiley.com/doi/10.1111/mec.70555 by Uppsala University Library, Wiley Online Library on [20/10/2026]. See the Terms and Conditions (https://onlinelibrary.wiley.com/terms-and-conditions) on Wiley Online Library for rules of use; OA articles are governed by the applicable Creative Commons License

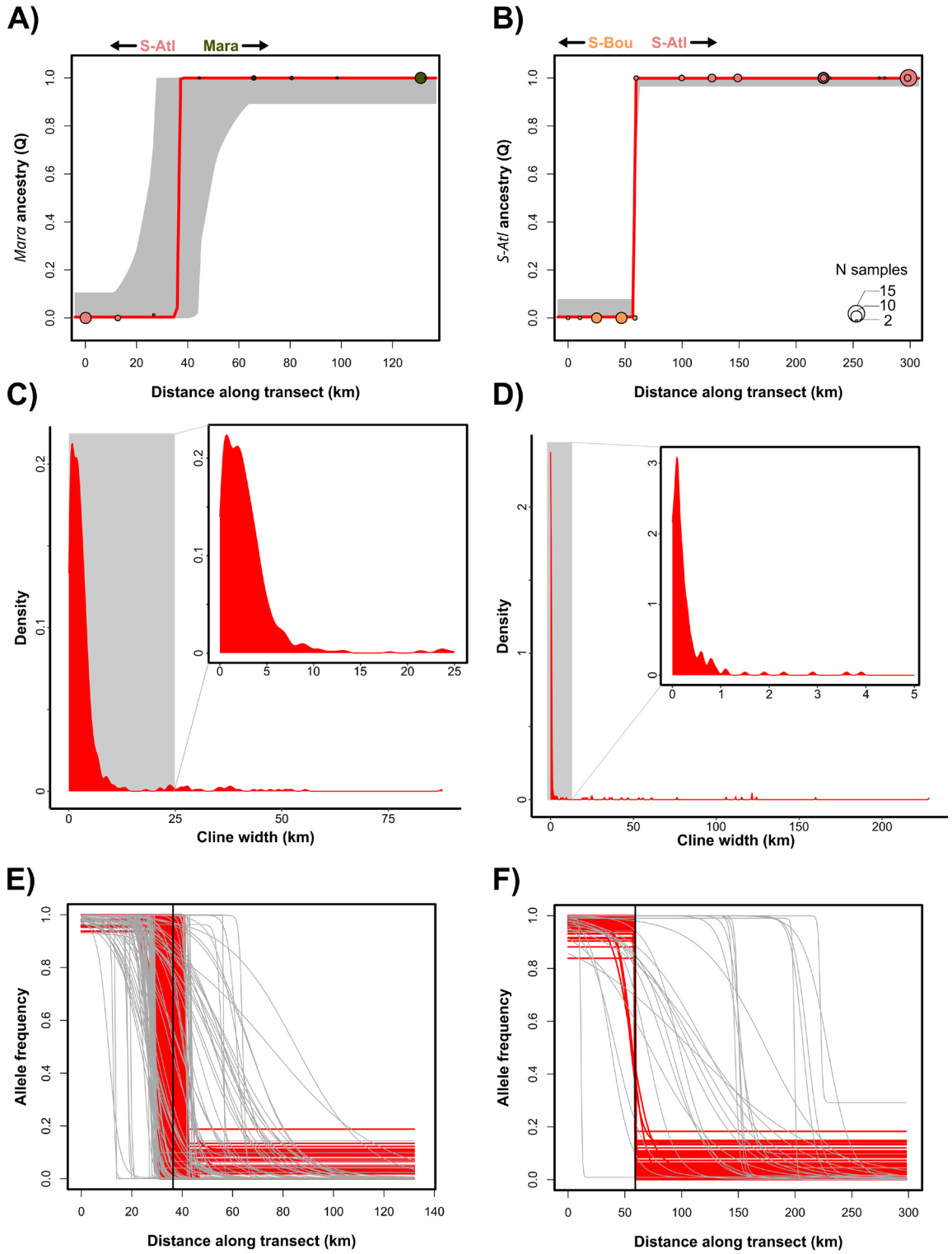

FIGURE 3 | Geographic cline analyses of the two transects: (A, C, E) from S-Atl to Mara and (B, D, F) from S-Bou to S-Atl. (A, B) Clines fitted to ancestry estimates (STRUCTURE Q values). Grey enveloppes denote 95% confidence intervals. The dots show the position of the sampling localities along the transects, scaled to sampling size. (C, D) Density distributions of cline width at single SNPs (including outliers). (E, F) Plots of sigmoid clines at single SNPs (grey: Outlier clines, red: Clines within two standard deviations of the distribution of cline parameters). The vertical black line shows the location of the centre of the ancestry clines.

uncertainty (confidence interval [CI] = 0–39.72 km). The cline centre was located 36.38 km from the Atlantic coast (CI = 24.11–48.19 km), falling in the middle of the sampling gap between the nearest localities assigned to either *S-Atl* or *Mara*. Note that we detected only minimal signal of admixture in the *S-Atl* side of the sampling gap (Figure 2B). A simple sigmoid cline also best fitted allele frequency at all 734 diagnostic SNPs (Figure 3C,E). Mean cline width was 3.84 km

1365294x, 2026, 19, Downloaded from https://onlinelibrary.wiley.com/doi/10.1111/mec.70555 by Uppsala University Library, Wiley Online Library on [20/10/2026]. See the Terms and Conditions (https://onlinelibrary.wiley.com/terms-and-conditions) on Wiley Online Library for rules of use; OA articles are governed by the applicable Creative Commons License

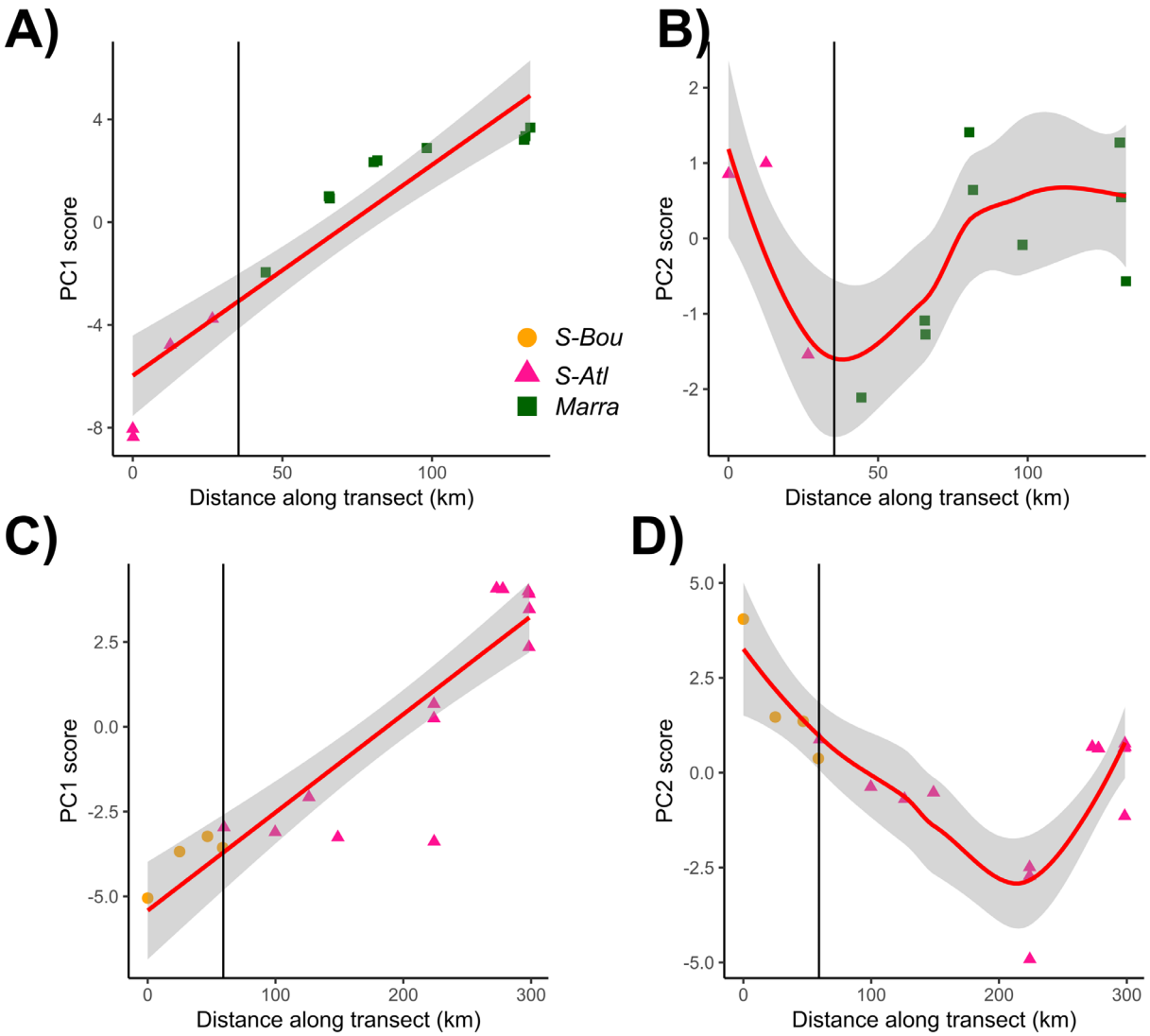

FIGURE 4 | Variation in bioclimatic variables along the two gradients. Changes of PC1 and PC2 scores of Principal Component Analyses based on 19 Bioclim variables along the S-Atl to Mara (A, B) and S-Bou to S-Atl (C, D) transects. The dots show localities (coloured according to the lineage they belong to) and the vertical black lines show the location of the centres of genomic ancestry clines. In A and C, the red line shows a linear regression fitted to the data, with the grey envelope showing the confidence interval around the slope and intercept. In C and D we fitted local regressions (loess) instead.

(5% quantile = 0.20 km; 95% quantile = 9.40 km), and mean cline centre 35.45 km (5% quantile = 27.72 km; 95% quantile = 41.80 km). The clines were overall consistent, with 605 out of 734 SNPs (82.43%) supporting a cline width and centre ± one standard deviation of the respective distributions (width: −3.71–11.66 km; centre: 29.41–41.66 km, Figure 4E). When omitting outlier clines with width or centre outside these intervals, mean cline width and centre were 2.36 and 35.52 km, respectively. Among the outliers, a cluster of SNPs supported narrower clines with a centre shifted towards *S-Atl* (Figure 3E).

Q values along the *S-Bou—S-Atl* transect also followed a simple cline, with an estimated width of 0.11 km (CI = 1.54×10^{-5}, 2.21 km, Figure 3B) and a centre located 59.26 km from the start of the transect (CI = 58.69–59.65 km), which corresponds to the mouth of the Oum Er R'bia River. Allele frequencies at 220 diagnostic SNPs were also best modelled by simple clines (Figure 3D,F), with a mean width of 7.81 km (5% quantile = 0 km; 95% quantile = 53.41 km) and mean centre at 66.78 km (5% quantile = 58.70 km; 95% quantile = 122.49 km). These results were strongly driven by a few outliers. When focusing on clines within ± one standard deviation of the distribution of cline parameters (189 of 220 diagnostic SNPs, 85.91%), the mean width was 0.64 km and the mean centre 59.06 km. Outlier clines were mostly shifted towards *S-Atl* (Figure 3F).

3.5 | Variation of Environmental Variables Along the Transects and Isolation by Environment

Along both transects, the first axis of the PCAs of 19 bioclimatic variables explained the majority of the climatic variation across localities (*Mara—S-Atl*: 88.30% of variance explained; *S-Bou—S-Atl*: 63.71%). These axes captured linear changes of climatic conditions according to latitude and longitude (Figure 4A,C; *S-Bou—S-Atl*: correlation between PC1 score and latitude: $R^2 = -0.91$, Pearson's product–moment correlation

1365294x, 2026, 19, Downloaded from https://onlinelibrary.wiley.com/doi/10.1111/mec.70555 by Uppsala University Library, Wiley Online Library on [20/10/2026]. See the Terms and Conditions (https://onlinelibrary.wiley.com/terms-and-conditions) on Wiley Online Library for rules of use; OA articles are governed by the applicable Creative Commons License

$p = 6.97 \times 10^{-8}$, correlation between PC1 score and longitude: $R^2 = -0.90$, $p = 1.14 \times 10^{-7}$; *Mara—S-Atl*: correlation between PC1 score and latitude: $R^2 = -0.87$, Pearson's product–moment correlation $p = 1.25 \times 10^{-5}$, correlation between PC1 score and longitude: $R^2 = 0.91$, $p = 7.97 \times 10^{-7}$) and were correlated to most bioclimatic variables (Figures S9 and S10). In the *S-Atl—Mara* transect, PC2 and PC3 explained 6.86% and 2.66% of the variance, respectively. Scores on these axes showed an inflection around the cline centre (Figure 4B, Figure S11) but did not clearly separate *S-Atl* and *Mara* localities. Indeed, the climatic disparity (measured as the distribution of pairwise distance on a PCA axis between sampling localities) was not higher between groups than within groups (Figure S12; PC2: Wilcoxon rank sum test $p > 0.98$, PC3: $p > 0.97$). Along the *S-Bou—S-Atl* transect, PC2 and PC3 explained 18.85% and 12.24% of the variance, respectively, and showed more discernible trends than in the first transect. PC2 scores decreased linearly from the northernmost localities south to the mouth of the Oued Tensift, before increasing again in the southernmost localities (Essaouira, Souira, Figure 2D). PC3 scores showed an inflection that roughly matched the centre of the *S-Bou—S-Atl* ancestry cline (Figure S13). However, climatic disparity again was not higher between lineages than within lineages (Figure S14; PC2: Wilcoxon rank sum test $p > 0.11$, PC3: $p = 1$). Multiple regressions on distance matrices revealed no significant contribution of the environment on genetic differentiation (Text S2, Table S2).

3.6 | Phylogenetic Reconstruction and Divergence Time Estimation

Phylogenetic inferences based on the concatenation of the loci in Assembly 2 with four missing data thresholds (60%, 40%, 20%, and 10% of missing data allowed) yielded a single, highly supported topology, with all internal nodes (i.e., crown of the mtDNA lineages and deeper) receiving an approximate likelihood ratio test support > 97%. The filtering strategy had a slight impact on split time estimates, with the age of older nodes increasing, and that of younger nodes decreasing, with more stringent filtering. However, the 95% confidence intervals of the four analyses largely overlapped (Table S3). Because over-filtering loci with missing data may have a negative impact on phylogenetic inference (Crotti et al. 2019; Huang and Knowles 2016), we refer to the results obtained from the matrix with the most permissive filter for the remainder of the paragraph. Our topology (Figure 5) is concordant with previous analyses in splitting the *A. erythrurus* complex into two main lineages: the Ibero-Moroccan clade on the one hand (the Moroccan lineages *S-Bou*, *S-Yah*, *S-Atl*, *Mara*, *Mid-Atl*, *M-Bou*, *N-Atl* and *Rif* and the Iberian lineage *Iberia* in Figure 5) and three lineages from Algeria and Tunisia (Algero-Tunisia, Central Algeria and *A. blanci* in Figure 5) on the other hand. These lineages split 12.02 million years ago (Mya; confidence interval (CI) = 10.17–13.95), and the crown of the Ibero-Moroccan clade was estimated at 6.93 Mya (CI = 6.50–7.64). The latter clade was subdivided into two main groups: the far north of Morocco (*Rif*, *N-Atl*) together with the Iberian populations, and the remaining of the Moroccan populations (all the Atlantic coast from Larache southwards, and the inland lineages of *Mid-Atl* and *Mara*). Within the latter, our focal lineages *Mara*, *S-Atl* and *S-Bou* were grouped in a clade originating 4.53 Mya (CI = 4.00–5.07). *Mara* and *S-Atl* were inferred as sister lineages (split time 4.36 Mya, CI = 3.85–5.01), while *S-Bou* was sister to *S-Yah*, a lineage distributed along the Atlantic coast north of Casablanca (split time 3.72 Mya, CI = 3.25–4.23).

4 | Discussion

Using genome-wide SNPs, we investigated intrinsic and extrinsic drivers of phylogeographic breaks in a small terrestrial vertebrate. Our results illustrate the challenge laid by accurately inferring phylogeographic breaks with pre-genomic datasets, even in the case of deep lineage splits (4.5 Mya in our case). A previous phylogeographic study of *Acanthodactylus erythrurus* in south-western Morocco, based on nine nuclear loci (Rancilhac et al. 2023), identified only one phylogeographic break (between the inland *Mara* lineage and the Atlantic coast) and suggested that all populations along the Atlantic coast were part of a single IBD gradient. Contrastingly, the genomic data we presented here, coupled with denser sampling, uncovered three well-separated, allopatric evolutionary lineages in the same area: *S-Atl* and *S-Bou* segregate latitudinally along a rather narrow coastal strip, while *Mara* ranges inland around Marrakech. Interestingly, RADseq data here recovers the same lineages as mtDNA (see Rancilhac et al. 2023), further emphasizing that marker informativeness is paramount to properly identify phylogeographic breaks and species boundaries (Doniol-Valcroze et al. 2024).

While intra-lineage genetic differentiation appears mainly driven by isolation by distance (IBD), we found unambiguous evidence of phylogeographic breaks separating lineages, a clear sign of past vicariance. Where these lineages meet, we inferred very steep transitions in ancestries with a virtual absence of admixture. Remarkably, while *S-Atl* and *S-Bou* are separated by the Ourm Er R'bia, a large river, the transition from *Mara* to *S-Atl* is not characterized by landscape features that could prevent migration. This pattern begs the question of what processes play out in the maintenance of phylogeographic breaks at the landscape level.

4.1 | Landscape-Level Barriers to Migration Are Not Necessary to Maintain Phylogeographic Breaks

The centre of the cline between the *S-Atl* and *S-Bou* lineages coincides with the mouth of the Ourm Er R'bia river. It thus seems likely that the river contributes to the phylogeographic pattern by reducing migration, either as a barrier responsible for the actual vicariance event or as a zone of reduced dispersal where tension zones tend to position themselves (Nichols 1989). Phylogeographic evidence suggests that rivers are important barriers to migration in many regions of the globe for small terrestrial vertebrates, including reptiles (Gonçalves-Sousa et al. 2022; Pellegrino et al. 2005; Pirani et al. 2019), amphibians (Goudarzi et al. 2019), and mammals, although they are sometimes permeable (Fonseca et al. 2024; Roratto et al. 2015). Interestingly, two permanent rivers cut through the range of *S-Atl*, without perceptible effect on population structure: the Oued Tensift reaching the sea at Souira and the Oued Ksob reaching the sea at Essaouira. Instead, our results suggest rather strong dispersal and gene flow within *S-Atl*: the isolation by distance

1365294x, 2026, 19, Downloaded from https://onlinelibrary.wiley.com/doi/10.1111/mec.70555 by Uppsala University Library, Wiley Online Library on [20/10/2026]. See the Terms and Conditions (https://onlinelibrary.wiley.com/terms-and-conditions) on Wiley Online Library for rules of use; OA articles are governed by the applicable Creative Commons License

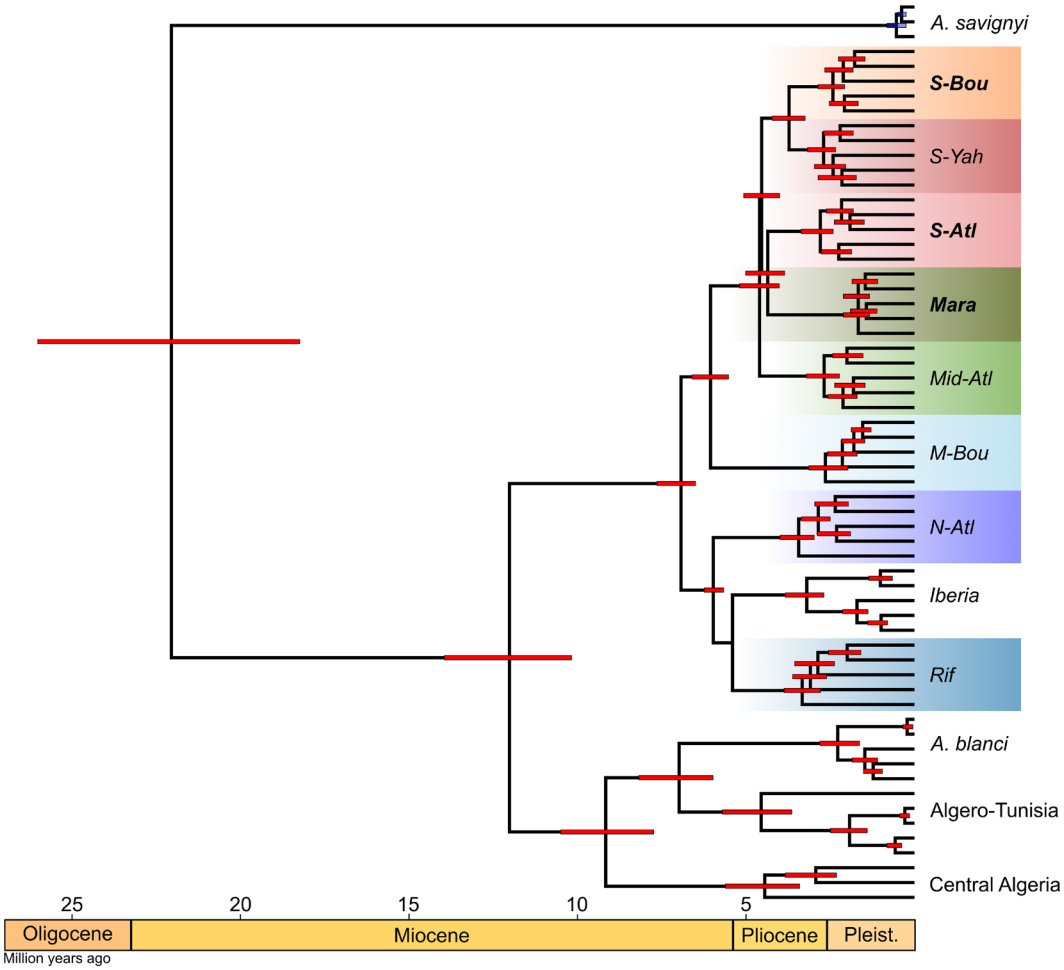

FIGURE 5 | Calibrated phylogeny of the *Acanthodactylus erythrurus* radiation, including 61 samples covering nine mtDNA lineages within the Ibero-Moroccan clade (colours matching those in Figure 1; the three focal lineages of the present study are indicated in bold), three lineages in Algeria and Tunisia and the outgroup A. savignyi. Red bars at the nodes indicate 95% confidence intervals around the time estimates. All internal nodes (i.e., crown of the lineages and lower) received a 100% approximate likelihood ratio test support.

slope, which is inversely proportional to dispersal distance (Rousset 1997), is weak, and nucleotide diversity is stable across localities, suggesting demographic equilibrium. The population structure that we detected within *S-Atl* was only supported by the first two axes of the PCA (explaining 6.06% of total variance) and matched large sampling gaps rather than barriers to migration. Thus, the Ourm Er R'bia appears as the only contemporary landscape feature that prevents migration and generates phylogeographic structure along the Atlantic coast. It is possible that the other aforementioned rivers are not wide enough to constrain migration or dry up during the summer. Indeed, satellite imagery suggests that both are partially dry 3 to 6 km upstream of their estuaries at least part of the year (Airbus CNES/Airbus Landsat imagery 2025, consulted 02/2025). Contrastingly, the Oum Er R'bia holds water far inland, except at its very mouth where the banks are connected by a sand bank.

In stark contrast, the transition between *S-Atl* and *Mara* does not coincide with a clear barrier to migration as our transect crosses continuous meso-xeric habitats inland along the Oued Tensift valley (see above). An alternative hypothesis is that the phylogeographic break coincides with a steep environmental transition, restraining gene flow between locally adapted lineages (Abbott and Brennan 2014; McCulloch et al. 2019; Ryan et al. 2017). We tested this hypothesis by investigating whether sudden changes in bioclimatic variables coincided with the two ancestry clines. We found that most of the environmental variation along both transects reflected linear, latitudinal gradients. In either case, we did not identify environmental variables exhibiting a sharp transition at the cline centre. Local adaptation could contribute to maintaining phylogeographic breaks in two ways. Firstly, it could generate prezygotic reproductive isolation if the two lineages were segregated by habitat and did not meet. However, environmental variables at localities on either side of the *S-Atl–Mara* cline were more similar to each other than localities within *S-Atl*, demonstrating that the latter is not strongly adapted to environmental conditions differing from that in *Mara*. Secondly, genetic divergence could be maintained by local adaptation if hybrids were maladapted to either environment and selected against (Muirhead and Presgraves 2016). However, this would also require a steep environmental transition, contrasting with our findings. Furthermore, our single-SNP clines demonstrate that many loci resist introgression, making it unlikely that they are all under strict and similar environmental local selection. Thus, local adaptation cannot explain the location of the phylogeographic break between *S-Atl* and *Mara*, and the steep transitions in both ancestry and allele frequencies.

1365294x, 2026, 19, Downloaded from https://onlinelibrary.wiley.com/doi/10.1111/mec.70555 by Uppsala University Library, Wiley Online Library on [20/10/2026]. See the Terms and Conditions (https://onlinelibrary.wiley.com/terms-and-conditions) on Wiley Online Library for rules of use; OA articles are governed by the applicable Creative Commons License

The two *A. erythrurus* phylogeographic breaks in Southern Morocco are interesting as they present similar patterns of genetic differentiation (i.e., similar split times, lack of admixture near contact zones, similar degrees of genetic differentiation) regardless of the presence of landscape features that might reduce migration. This demonstrates that, while geographical barriers may contribute to phylogeographic patterns, other key factors underlie their origin and maintenance.

4.2 | Narrow Geographic Clines Suggest Intrinsic Reproductive Isolation Across Lineages

Owing to the lack of admixture along both transects, geographic clines fitted to ancestry estimates were extremely narrow. Hundreds of unlinked diagnostic SNPs also supported clines consistent with the ancestry cline. Such a pattern is typical of tension zones, where hybrids are counter-selected (Abbott 2017; Gay et al. 2008). In this case, cline width depends on a balance between selection against hybrids and dispersal (Szymura and Barton 1986). We describe clines with widths ranging from 0.6 to 4 km, suggesting either very strong selection against hybrids or very small dispersal abilities. As we argued above, the latter seems unlikely considering the lack of strong within-lineages structure and the weakness of isolation by distance slopes. In amphibians, narrow single-SNP clines, with widths following a Poisson distribution near zero as we found here, are typical of species pairs with strong reproductive isolation (Dufresnes et al. 2021). Furthermore, the lack of introgression tails in the single-SNP clines supports the lack of neutral introgression at diagnostic SNPs (Szymura and Barton 1986).

One caveat of our study is that we did not find 'true' sympatric localities (i.e., where both lineages were found to co-occur). Between *S-Atl* and *S-Bou*, the closest localities are ~1 km apart, but the Oum Er R'bia river between them probably acts as a strong barrier to migration. In this case, cline width would not measure selection against hybrids. However, satellite imagery reveals that the river's mouth is dry at least intermittently (Airbus CNES/Airbus Landsat imagery 2025, consulted 02/2025), allowing in theory dispersal across the barrier and hence hybridization. This idea is also supported by a few diagnostic SNPs with wide clines, although these may represent stochastic variation in the distribution. Between *S-Atl* and *Mara*, the cline centre coincides with an 18.7 km sampling gap, which probably explains the higher uncertainty around cline parameter estimates. If this gap corresponds to an actual discontinuity in their distribution that is larger than dispersal abilities, we cannot evaluate reproductive isolation. However, remnant habitat patches are distributed continuously along the Oued Tensift (P.-A.C., pers. obs.), suggesting that *A. erythrurus* still occurs, or occurred recently, in the area corresponding to the sampling gap. In this region, *A. erythrurus* populations are largely restricted to patches of alluvial natural habitats along the river (P.-A.C., pers. obs.) that are separated by cultivated fields, but must have been more extensive and (nearly) continuous before the recent expansion of agriculture in the area between Marrakech and the Atlantic coast. Of note, we detected a cluster of narrow single-SNP clines with a centre shifted towards *S-Atl*, suggestive of hybrid zone movement (Wielstra 2019). Thus, it is likely that individuals of the *S-Atl* and *Mara* lineages were able to interact at least until recently. In the absence of strong reproductive barriers, traces of admixture should therefore be detectable. Surprisingly, we detected higher levels of introgression in an isolated locality at the southern range of *Mara*, suggesting the existence of another hybrid zone. Unless we sampled the centre of the hybrid zone by chance, the higher levels of admixture there suggest that introgression rates between *S-Atl* and *Mara* are higher than in the transect. This could mean that reproductive isolation is partially driven by extrinsic factors (e.g., population density, environmental factors). However, it should be noted that ghost introgression (i.e., introgression from an additional, unsampled lineage) may yield spurious results in STRUCTURE analyses (Lawson et al. 2018). Thus, we refrain from further interpretations of this pattern in the absence of additional sampling.

Overall, our geographic cline analyses support the presence of intrinsic reproductive barriers between *S-Atl* and *Mara* and *S-Atl* and *S-Bou*. We inferred split times of 4.3–4.5 Mya, a divergence time sufficient for near-complete reproductive isolation to evolve in amphibians (Dufresnes et al. 2015) and similar to split time between other lacertid lizard species with narrow tension zones (Caeiro-Dias et al. 2021; Kornilios et al. 2019, 2020). The nature of these barriers remains unresolved. The large amount of loci supporting narrow clines suggest a highly polygenic basis for reproductive isolation (Dufresnes et al. 2021). However, large-effect loci may disproportionately contribute to speciation. Karyotype analyses have revealed that *S-Atl* and *Mara* strongly differ in the morphology of their Z chromosome (P. A. Crochet, F. Veyrunes, *in prep.*), which may largely contribute to hybrid dysfunctions (Irwin 2018; Payseur et al. 2018). In the absence of a reference genome, we did not try to determine whether the diagnostic SNPs are predominantly present on the Z chromosome. Autosomal barrier loci may also play an important role (Dufresnes et al. 2021), particularly if reinforcement mechanisms are in place in hybrid zones (Nosil et al. 2003; Pfennig and Rice 2014).

4.3 | Implications for the Systematics of *Acanthodactylus erythrurus*

The high levels of genetic divergence and lack of introgression across *S-Atl, S-Bou* and *Mara* strongly suggest that these lineages represent separate species under the biological species concept (as refined by e.g., Dufresnes et al. (2023) or Schweizer et al. (2023)). The geographical boundaries of *S-Atl* and *Mara* should be clear: *S-Atl* is surrounded by the two other lineages except in the south where it marks the southern limit of the range of *A. erythrurus*, while the closest populations to *Mara* in the north-east (Middle-Atlas and High-Atlas) are clearly differentiated genetically and morphologically (Miralles et al. 2020; Rancilhac et al. 2023). The northern limit of *S-Bou*, however, is unclear as our phylogenetic reconstruction suggests that it is closely related to the *S-Yah* mitochondrial lineage. A comprehensive study of *A. erythrurus* based on genome-wide SNPs will be required to delineate and formally name all species-level lineages within the complex, but our results further confirm that it is a continental radiation of many cryptic species (Doniol-Valcroze et al. 2024; Miralles et al. 2020). Furthermore, our phylogenetic analysis shows that most mitochondrial lineages within the IM clade are well supported by genomic data and may represent vicariant lineages, contrary to previous conclusions (Rancilhac et al. 2023).

1365294x, 2026, 19, Downloaded from https://onlinelibrary.wiley.com/doi/10.1111/mec.70555 by Uppsala University Library, Wiley Online Library on [20/10/2026]. See the Terms and Conditions (https://onlinelibrary.wiley.com/terms-and-conditions) on Wiley Online Library for rules of use; OA articles are governed by the applicable Creative Commons License

4.4 | Conclusions

In this study, we illustrated how phylogeographic results based on a few markers can be misleading when trying to identify independent evolutionary lineages resulting from past vicariance events and how genomic data increase our explanatory power. Genomic data uncovered three evolutionary lineages with evidence of intrinsic reproductive isolation in a restricted geographic area in SW Morocco. These findings support the role of speciation rather than extrinsic, purely geographical isolation in building biodiversity in these organisms. Our results also suggest that geographic barriers to gene flow and steep ecological gradients are not necessary to maintain phylogeographic breaks. We propose a model where ancestral range fragmentation led to allopatric divergence, with high ecological niche conservatism preventing the establishment of secondary sympatry. Intrinsic reproductive isolation plays an important role in maintaining lineage divergence, suggesting that time in isolation is a determining factor explaining the presence and steepness of phylogeographic breaks. It would be interesting to implement a comparative approach across various taxa to determine the extent to which this conclusion can be generalized. We expect that this pattern is organism- and region-specific to some extent because it relies on initial geological events separating the lineages and on sufficiently low dispersal abilities to reduce or interrupt gene flow over an extended period.

The reasons for the initial fragmentation of *A. erythrurus* remain an open question. The diversion of the Ourm Er R'bia river into its current bed between 4 and 5 Mya may have initiated the divergence of *S-Bou*, as it coincides with the split time estimated in our timetree analysis (Yaaqoub and Essaifi 2023). Furthermore, cycles of arid and humid periods have been recorded in the region since the upper Pliocene (Le Houérou 1997), which may have contributed to isolate *A. erythrurus* populations in refugia with wetter climates during more arid periods, as has been recorded during the Pleistocene in many North African mesic taxa (Brito et al. 2014). The *A. erythrurus* radiation is a promising system to understand the extrinsic and intrinsic factors underlying the build-up of biodiversity in Northern Africa.

Author Contributions

F.G.d.A.: prepared the data, analysed data, visualized results, wrote code, prepared figures, wrote the original draft, reviewed and edited the draft; L.R.: conceptualized the study, analysed data, visualized results, wrote code, prepared figures, wrote the original draft, reviewed and edited the draft; R.L.: provided computational resources, managed data, reviewed and edited the draft; L.B., A.L.: performed laboratory work; M.B., A.B., J.C.B., L.E.-M., A.M., S.C.: provided samples, performed fieldwork, reviewed and edited the draft; P.G.: managed samples, performed fieldwork, reviewed and edited the draft; P.-A.C.: acquired funding, managed the project, performed fieldwork, managed samples and data, conceptualized the study, reviewed and edited the draft.

Acknowledgements

The authors thank the collectors whose names appear in Table S3 as well as D. J. Harris and S. Carranza for sharing their samples and P. Doniol-Valcroze and C. Dufresnes for their help with analyses. Part of this work was carried out by using the resources of the national INRAe MIGALE (Migale bioinformatics Facility, https://doi.org/10.15454/1.5572390655343293E12) and GENOTOUL (Bioinfo Genotoul, https://doi.org/10.15454/1.5572369328961167E12) bioinformatics HPC platforms, as well as the local Montpellier Bioinformatics Biodiversity (MBB, supported by the LabEx CeMEB) and CBGP HPC platform services. Open access publication funding provided by COUPERIN CY26.

Funding

This project benefited from funding by the LabEx CEMeB to P-.-A.C. and by the Agence Nationale de la Recherche (MOHMIE ANR-09-PEXT-004) to P-.-A.C., A.M. and R.L.

Conflicts of Interest

The authors declare no conflicts of interest.

Data Availability Statement

The raw RADseq reads were deposited on the European Nucleotide Archive under project PRJEB115474. The input files and script necessary to reproduce the analyses are available on Zenodo under doi 10.5281/zenodo.17250188.

References

Abbott, R. J. 2017. "Plant Speciation Across Environmental Gradients and the Occurrence and Nature of Hybrid Zones." *Journal of Systematics and Evolution* 55, no. 4: 238–258. https://doi.org/10.1111/jse.12267.

Abbott, R. J., and A. C. Brennan. 2014. "Altitudinal Gradients, Plant Hybrid Zones and Evolutionary Novelty." *Philosophical Transactions of the Royal Society, B: Biological Sciences* 369, no. 1648: 20130346. https://doi.org/10.1098/rstb.2013.0346.

Audzijonyte, A., and R. C. Vrijenhoek. 2010. "When Gaps Really Are Gaps: Statistical Phylogeography of Hydrothermal Vent Invertebrates." *Evolution* 64, no. 8: 2369–2384. https://doi.org/10.1111/j.1558-5646.2010.00987.x.

Avise, J. C. 2000. *Phylogeography: The History and Formation of Species*. Harvard University Press.

Barton, N. H. 1979. "Gene Flow Past a Cline." *Heredity* 43, no. 3: 333–339. https://doi.org/10.1038/hdy.1979.86.

Barton, N. H., and G. M. Hewitt. 1985. "Analysis of Hybrid Zones." *Annual Review of Ecology, Evolution, and Systematics* 16: 113–148. https://doi.org/10.1146/annurev.es.16.110185.000553.

Bolger, A. M., M. Lohse, and B. Usadel. 2014. "Trimmomatic: A Flexible Trimmer for Illumina Sequence Data." *Bioinformatics* 30, no. 15: 2114–2120. https://doi.org/10.1093/bioinformatics/btu170.

Brito, J. C., R. Godinho, F. Martinez-Freiria, et al. 2014. "Unravelling Biodiversity, Evolution and Threats to Conservation in the Sahara-Sahel." *Biological Reviews* 89: 215–231. https://doi.org/10.1111/brv.12049.

Caeiro-Dias, G., S. Rocha, A. Couto, et al. 2021. "Nuclear Phylogenies and Genomics of a Contact Zone Establish the Species Rank of *Podarcis lusitanicus* (Squamata, Lacertidae)." *Molecular Phylogenetics and Evolution* 164: 107270. https://doi.org/10.1016/j.ympev.2021.107270.

Carné, A., and D. R. Vieites. 2024. "A Race Against Extinction: The Challenge to Overcome the Linnean Amphibian Shortfall in Tropical Biodiversity Hotspots." *Diversity and Distributions* 30, no. 12: e13912. https://doi.org/10.1111/ddi.13912.

Coyne, J. A., and A. Orr. 2004. *Speciation*. Sinauer.

Crotti, M., C. D. Barratt, S. P. Loader, D. J. Gower, and J. W. Streicher. 2019. "Causes and Analytical Impacts of Missing Data in RADseq Phylogenetics: Insights From an African Frog (*Afrixalus*)." *Zoologica Scripta* 48, no. 2: 157–167. https://doi.org/10.1111/zsc.12335.

13652294x, 2026, 19, Downloaded from https://onlinelibrary.wiley.com/doi/10.1111/mec.70555 by Uppsala University Library, Wiley Online Library on [20/10/2026]. See the Terms and Conditions (https://onlinelibrary.wiley.com/terms-and-conditions) on Wiley Online Library for rules of use; OA articles are governed by the applicable Creative Commons License

DeRaad, D. A. 2021. "RADstackshelpR: Optimize the De Novo Stacks Pipeline Via R." R Package Version 0.1.0. https://devonderaad.github.io/RADstackshelpR/index.html.

Derryberry, E. P., G. E. Derryberry, J. M. Maley, and R. T. Brumfield. 2014. "Hzar: Hybrid Zone Analysis Using an R Software Package." *Molecular Ecology Resources* 14, no. 3: 652–663. https://doi.org/10.1111/1755-0998.12209.

Doniol-Valcroze, P., L. Rancilhac, J.-C. Brito, et al. 2024. "Combining RADseq and Contact Zone Analysis to Decipher Cryptic Diversification in Reptiles: Insights From the Spiny-Footed Lizard (Reptilia, Lacertidae)." *Zoologica Scripta* 53, no. 1: 1–15. https://doi.org/10.1111/zsc.12628.

Dufresnes, C., A. Brelsford, J. Crnobrnja-Isailović, N. Tzankov, P. Lymberakis, and N. Perrin. 2015. "Timeframe of Speciation Inferred From Secondary Contact Zones in the European Tree Frog Radiation (*Hyla arborea* Group)." *BMC Evolutionary Biology* 15, no. 1: 155. https://doi.org/10.1186/s12862-015-0385-2.

Dufresnes, C., A. Brelsford, D. L. Jeffries, et al. 2021. "Mass of Genes Rather Than Master Genes Underlie the Genomic Architecture of Amphibian Speciation." *Proceedings of the National Academy of Sciences of the United States of America* 118, no. 36: e2103963118. https://doi.org/10.1073/pnas.2103963118.

Dufresnes, C., A. G. Nicieza, S. N. Litvinchuk, et al. 2020. "Are Glacial Refugia Hotspots of Speciation and Cytonuclear Discordances? Answers From the Genomic Phylogeography of Spanish Common Frogs." *Molecular Ecology* 29, no. 5: 986–1000. https://doi.org/10.1111/mec.15368.

Dufresnes, C., N. Poyarkov, and D. Jablonski. 2023. "Acknowledging More Biodiversity Without More Species." *Proceedings of the National Academy of Sciences of the United States of America* 120: e2302424120. https://doi.org/10.1073/pnas.2302424120.

Dufresnes, C., M. Pribille, B. Alard, et al. 2020. "Integrating Hybrid Zone Analyses in Species Delimitation: Lessons From Two Anuran Radiations of the Western Mediterranean." *Heredity* 124, no. 3: 423–438. https://doi.org/10.1038/s41437-020-0294-z.

Earl, D. A., and B. M. vonHoldt. 2012. "STRUCTURE HARVESTER: A Website and Program for Visualizing STRUCTURE Output and Implementing the Evanno Method." *Conservation Genetics Resources* 4, no. 2: 359–361. https://doi.org/10.1007/s12686-011-9548-7.

Evanno, G., S. Regnaut, and J. Goudet. 2005. "Detecting the Number of Clusters of Individuals Using the Software Structure: A Simulation Study." *Molecular Ecology* 14, no. 8: 2611–2620. https://doi.org/10.1111/j.1365-294X.2005.02553.x.

Ficetola, G. F., A. Bonardi, R. Sindaco, and E. Padoa-Schioppa. 2013. "Estimating Patterns of Reptile Biodiversity in Remote Regions." *Journal of Biogeography* 40, no. 6: 1202–1211. https://doi.org/10.1111/jbi.12060.

Fick, S. E., and R. J. Hijmans. 2017. "WorldClim 2: New 1-Km Spatial Resolution Climate Surfaces for Global Land Areas." *International Journal of Climatology* 37, no. 12: 4302–4315. https://doi.org/10.1002/joc.5086.

Fonseca, E. M., N. S. Pope, W. E. Peterman, F. P. Werneck, G. R. Colli, and B. C. Carstens. 2024. "Genetic Structure and Landscape Effects on Gene Flow in the Neotropical Lizard *Norops brasiliensis* (Squamata: Dactyloidae)." *Heredity* 132: 284–295. https://doi.org/10.1038/s41437-024-00682-5.

Fonseca, M. M., J. C. Brito, O. S. Paulo, M. A. Carretero, and D. J. Harris. 2009. "Systematic and Phylogeographical Assessment of the *Acanthodactylus erythrurus* Group (Reptilia: Lacertidae) Based on Phylogenetic Analyses of Mitochondrial and Nuclear DNA." *Molecular Phylogenetics and Evolution* 51, no. 2: 131–142. https://doi.org/10.1016/j.ympev.2008.11.021.

Garrick, R. C., J. D. Banusiewicz, S. Burgess, C. Hyseni, and R. E. Symula. 2019. "Extending Phylogeography to Account for Lineage Fusion." *Journal of Biogeography* 46, no. 2: 268–278. https://doi.org/10.1111/jbi.13503.

Gay, L., P.-A. Crochet, D. A. Bell, and T. Lenormand. 2008. "Comparing Clines on Molecular and Phenotypic Traits in Hybrid Zones: A Window on Tension Zone Models." *Evolution* 62, no. 11: 2789–2806. https://doi.org/10.1111/j.1558-5646.2008.00491.x.

Gonçalves-Sousa, J. G., R. de Fraga, B. S. Menezes, D. O. Mesquita, and R. W. Ávila. 2022. "Riverine Barrier and Aridity Effects on Taxonomic, Phylogenetic and Functional Diversities of Lizard Assemblages From a Semi-Arid Region." *Journal of Biogeography* 49, no. 6: 1021–1033. https://doi.org/10.1111/jbi.14356.

Goudarzi, F., M.-R. Hemami, L. Rancilhac, et al. 2019. "Geographic Separation and Genetic Differentiation of Populations Are Not Coupled With Niche Differentiation in Threatened Kaiser's Spotted Newt (*Neurergus kaiseri*)." *Scientific Reports* 9: 6239. https://doi.org/10.1038/s41598-019-41886-8.

Grossenbacher, D. L., S. D. Veloz, and J. P. Sexton. 2014. "Niche and Range Size Patterns Suggest That Speciation Begins in Small, Ecologically Diverged Populations in North American Monkeyflowers (*Mimulus* spp.)." *Evolution* 68, no. 5: 1270–1280. https://doi.org/10.1111/evo.12355.

Guindon, S., J.-F. Dufayard, V. Lefort, M. Anisimova, W. Hordijk, and O. Gascuel. 2010. "New Algorithms and Methods to Estimate Maximum-Likelihood Phylogenies: Assessing the Performance of PhyML 3.0." *Systematic Biology* 59, no. 3: 307–321. https://doi.org/10.1093/sysbio/syq010.

Harris, D. J., D. Sergiadou, and J. F. Faria. 2024. "New Data on the Diversity and Distribution of Lineages of the *Acanthodactylus erythrurus* Species Complex in North Africa Derived From Mitochondrial DNA Markers." *Herpetozoa* 37: 281–286. https://doi.org/10.3897/herpetozoa.37.e118175.

Hausdorf, B., and C. Hennig. 2020. "Species Delimitation and Geography." *Molecular Ecology Resources* 20, no. 4: 950–960. https://doi.org/10.1111/1755-0998.13184.

Hortal, J., F. de Bello, J. A. F. Diniz-Filho, T. M. Lewinsohn, J. M. Lobo, and R. J. Ladle. 2015. "Seven Shortfalls That Beset Large-Scale Knowledge of Biodiversity." *Annual Review of Ecology, Evolution, and Systematics* 46: 523–549. https://doi.org/10.1146/annurev-ecolsys-112414-054400.

Huang, H., and L. L. Knowles. 2016. "Unforeseen Consequences of Excluding Missing Data From Next-Generation Sequences: Simulation Study of RAD Sequences." *Systematic Biology* 65, no. 3: 357–365. https://doi.org/10.1093/sysbio/syu046.

Irwin, D. E. 2002. "Phylogeographic Breaks Without Barriers to Gene Flow." *Evolution* 56, no. 12: 2383–2394. https://doi.org/10.1111/j.0014-3820.2002.tb00164.x.

Irwin, D. E. 2018. "Sex Chromosomes and Speciation in Birds and Other ZW Systems." *Molecular Ecology* 27, no. 19: 3831–3851. https://doi.org/10.1111/mec.14537.

Jakobsson, M., and N. A. Rosenberg. 2007. "CLUMPP: A Cluster Matching and Permutation Program for Dealing With Label Switching and Multimodality in Analysis of Population Structure." *Bioinformatics* 23, no. 14: 1801–1806. https://doi.org/10.1093/bioinformatics/btm233.

Kalyaanamoorthy, S., B. Q. Minh, T. K. F. Wong, A. von Haeseler, and L. S. Jermiin. 2017. "ModelFinder: Fast Model Selection for Accurate Phylogenetic Estimates." *Nature Methods* 14, no. 6: 587–589. https://doi.org/10.1038/nmeth.4285.

13652294x, 2026, 19, Downloaded from https://onlinelibrary.wiley.com/doi/10.1111/mec.70555 by Uppsala University Library, Wiley Online Library on [20/10/2026]. See the Terms and Conditions (https://onlinelibrary.wiley.com/terms-and-conditions) on Wiley Online Library for rules of use; OA articles are governed by the applicable Creative Commons License

Knaus, B. J., and N. J. Grünwald. 2017. "Vcfr: A Package to Manipulate and Visualize Variant Call Format Data in R." *Molecular Ecology Resources* 17, no. 1: 44–53. https://doi.org/10.1111/1755-0998.12549.

Kornilios, P., E. Thanou, P. Lymberakis, Ç. Ilgaz, Y. Kumlutaş, and A. Leaché. 2019. "Genome-Wide Markers Untangle the Green-Lizard Radiation in the Aegean Sea and Support a Rare Biogeographical Pattern." *Journal of Biogeography* 46, no. 3: 552–567. https://doi.org/10.1111/jbi.13524.

Kornilios, P., E. Thanou, P. Lymberakis, Ç. Ilgaz, Y. Kumlutaş, and A. Leaché. 2020. "A Phylogenomic Resolution for the Taxonomy of Aegean Green Lizards." *Zoologica Scripta* 49, no. 1: 14–27. https://doi.org/10.1111/zsc.12385.

Krijgsman, W., F. J. Hilgen, I. Raffi, F. J. Sierro, and D. S. Wilson. 1999. "Chronology, Causes and Progression of the Messinian Salinity Crisis." *Nature* 400, no. 6745: 652–655. https://doi.org/10.1038/23231.

Kuo, C.-H., and J. C. Avise. 2005. "Phylogeographic Breaks in Low-Dispersal Species: The Emergence of Concordance Across Gene Trees." *Genetica* 124, no. 2: 179–186. https://doi.org/10.1007/s10709-005-2095-y.

Lawson, D. J., L. van Dorp, and D. Falush. 2018. "A Tutorial on How Not to Over-Interpret STRUCTURE and ADMIXTURE Bar Plots." *Nature Communications* 9, no. 1: 3258. https://doi.org/10.1038/s41467-018-05257-7.

Le Houérou, H. N. 1997. "Climate, Flora and Fauna Changes in the Sahara Over the Past 500 Million Years." *Journal of Arid Environments* 37, no. 4: 619–647. https://doi.org/10.1006/jare.1997.0315.

Leaché, A. D., J. R. Oaks, C. Ofori-Boateng, and M. K. Fujita. 2020. "Comparative Phylogeography of West African Amphibians and Reptiles." *Evolution* 74, no. 4: 716–724. https://doi.org/10.1111/evo.13941.

McCulloch, G. A., B. J. Foster, L. Dutoit, et al. 2019. "Ecological Gradients Drive Insect Wing Loss and Speciation: The Role of the Alpine Treeline." *Molecular Ecology* 28, no. 13: 3141–3150. https://doi.org/10.1111/mec.15114.

Miralles, A., P. Geniez, M. Beddek, et al. 2020. "Morphology and Multilocus Phylogeny of the Spiny-Footed Lizard (*Acanthodactylus erythrurus*) Complex Reveal Two New Mountain Species From the Moroccan Atlas." *Zootaxa* 4747, no. 2: zootaxa.4747.2.4. https://doi.org/10.11646/zootaxa.4747.2.4.

Muirhead, C. A., and D. C. Presgraves. 2016. "Hybrid Incompatibilities, Local Adaptation, and the Genomic Distribution of Natural Introgression Between Species." *American Naturalist* 187, no. 2: 249–261. https://doi.org/10.1086/684583.

Nguyen, L.-T., H. A. Schmidt, A. von Haeseler, and B. Q. Minh. 2015. "IQ-TREE: A Fast and Effective Stochastic Algorithm for Estimating Maximum-Likelihood Phylogenies." *Molecular Biology and Evolution* 32, no. 1: 268–274. https://doi.org/10.1093/molbev/msu300.

Nichols, R. A. 1989. "The Fragmentation of Tension Zones in Sparsely Populated Areas." *American Naturalist* 134, no. 6: 969–977. https://doi.org/10.1086/285025.

Nosil, P., B. J. Crespi, and C. P. Sandoval. 2003. "Reproductive Isolation Driven by the Combined Effects of Ecological Adaptation and Reinforcement." *Proceedings of the Royal Society of London. Series B: Biological Sciences* 270, no. 1527: 1911–1918. https://doi.org/10.1098/rspb.2003.2457.

Paris, J. R., J. R. Stevens, and J. M. Catchen. 2017. "Lost in Parameter Space: A Road Map for Stacks." *Methods in Ecology and Evolution* 8, no. 10: 1360–1373. https://doi.org/10.1111/2041-210X.12775.

Payseur, B. A., D. C. Presgraves, and D. A. Filatov. 2018. "Introduction: Sex Chromosomes and Speciation." *Molecular Ecology* 27, no. 19: 3745–3748. https://doi.org/10.1111/mec.14828.

Peixoto, G. M., R. D. Fraga, M. C. Araújo, I. L. Kaefer, and A. P. Lima. 2020. "Hierarchical Effects of Historical and Environmental Factors on Lizard Assemblages in the Upper Madeira River, Brazilian Amazonia." *PLoS One* 15, no. 6: e0233881. https://doi.org/10.1371/journal.pone.0233881.

Pellegrino, K. C. M., M. T. Rodrigues, A. N. Waite, M. Morando, Y. Y. Yassuda, and J. W. Sites Jr. 2005. "Phylogeography and Species Limits in the *Gymnodactylus darwinii* Complex (Gekkonidae, Squamata): Genetic Structure Coincides With River Systems in the Brazilian Atlantic Forest." *Biological Journal of the Linnean Society* 85, no. 1: 13–26. https://doi.org/10.1111/j.1095-8312.2005.00472.x.

Perret, J., O. Cobelli, A. Taudière, et al. 2023. "Time to Refine the Geography of Biodiversity Hotspots by Integrating Molecular Data: The Mediterranean Basin as a Case Study." *Biological Conservation* 284: 110162. https://doi.org/10.1016/j.biocon.2023.110162.

Pfennig, K. S., and A. M. Rice. 2014. "Reinforcement Generates Reproductive Isolation Between Neighbouring Conspecific Populations of Spadefoot Toads." *Proceedings of the Royal Society B: Biological Sciences* 281, no. 1789: 20140949. https://doi.org/10.1098/rspb.2014.0949.

Pirani, R. M., F. P. Werneck, A. T. Thomaz, et al. 2019. "Testing Main Amazonian Rivers as Barriers Across Time and Space Within Widespread Taxa." *Journal of Biogeography* 46, no. 11: 2444–2456. https://doi.org/10.1111/jbi.13676.

Pounds, J. A., and J. F. Jackson. 1981. "Riverine Barriers to Gene Flow and the Differentiation of Fence Lizard Populations." *Evolution* 35, no. 3: 516–528. https://doi.org/10.2307/2408199.

Pritchard, J. K., M. Stephens, and P. Donnelly. 2000. "Inference of Population Structure Using Multilocus Genotype Data." *Genetics* 155, no. 2: 945–959. https://doi.org/10.1093/genetics/155.2.945.

Pritchard, J. K., X. Wen, and D. Falush. 2010. *Documentation for Structure Software: Version 2.3*. University of Chicago. https://web.stanford.edu/group/pritchardlab/structure_software/release_versions/v2.3.4/structure_doc.pdf.

R Core Team. 2023. *R: A Language and Environment for Statistical Computing*. R Foundation for Statistical Computing. https://www.R-project.org.

Rancilhac, L., A. Miralles, P. Geniez, et al. 2023. "Phylogeographic Breaks and How to Find Them: An Empirical Attempt at Separating Vicariance From Isolation by Distance in a Lizard With Restricted Dispersal." *Peer Community Journal* 3: e74. https://doi.org/10.24072/pcjournal.301.

Rochette, N. C., A. G. Rivera-Colón, and J. M. Catchen. 2019. "Stacks 2: Analytical Methods for Paired-End Sequencing Improve RADseq-Based Population Genomics." *Molecular Ecology* 28, no. 21: 4737–4754. https://doi.org/10.1111/mec.15253.

Roratto, P. A., F. A. Fernandes, and T. R. O. de Freitas. 2015. "Phylogeography of the Subterranean Rodent *Ctenomys torquatus*: An Evaluation of the Riverine Barrier Hypothesis." *Journal of Biogeography* 42, no. 4: 694–705. https://doi.org/10.1111/jbi.12460.

Rousset, F. 1997. "Genetic Differentiation and Estimation of Gene Flow From F-Statistics Under Isolation by Distance." *Genetics* 145, no. 4: 1219–1228. https://doi.org/10.1093/genetics/145.4.1219.

Ruegg, K. 2008. "Genetic, Morphological, and Ecological Characterization of a Hybrid Zone That Spans a Migratory Divide." *Evolution* 62, no. 2: 452–466. https://doi.org/10.1111/j.1558-5646.2007.00263.x.

Ryan, S. F., M. C. Fontaine, J. M. Scriber, M. E. Pfrender, S. T. O'Neil, and J. J. Hellmann. 2017. "Patterns of Divergence Across the Geographic and Genomic Landscape of a Butterfly Hybrid Zone Associated With a Climatic Gradient." *Molecular Ecology* 26, no. 18: 4725–4742. https://doi.org/10.1111/mec.14236.

Schluter, D. 2009. "Evidence for Ecological Speciation and Its Alternative." *Science* 323, no. 5915: 737–741. https://doi.org/10.1126/science.1160006.

1365294x, 2026, 19, Downloaded from https://onlinelibrary.wiley.com/doi/10.1111/mec.70555 by Uppsala University Library, Wiley Online Library on [20/10/2026]. See the Terms and Conditions (https://onlinelibrary.wiley.com/terms-and-conditions) on Wiley Online Library for rules of use; OA articles are governed by the applicable Creative Commons License

Schweizer, M., D. A. Marques, U. Olsson, and P.-A. Crochet. 2023. "The Howard & Moore Complete Checklist of the Birds of the World: Framework for Species Delimitation." *Avian Systematics* 1: N35–N41.

Stankowski, S., A. D. Cutter, I. Satokangas, et al. 2024. "Toward the Integration of Speciation Research." *Evolutionary Journal of the Linnean Society* 3, no. 1: kzae001. https://doi.org/10.1093/evolinnean/kzae001.

Stankowski, S., and M. Ravinet. 2021. "Defining the Speciation Continuum." *Evolution* 75, no. 6: 1256–1273. https://doi.org/10.1111/evo.14215.

Stekhoven, D. J., and P. Bühlmann. 2012. "MissForest—Non-Parametric Missing Value Imputation for Mixed-Type Data." *Bioinformatics* 28, no. 1: 112–118. https://doi.org/10.1093/bioinformatics/btr597.

Struck, T. H., J. L. Feder, M. Bendiksby, et al. 2018. "Finding Evolutionary Processes Hidden in Cryptic Species." *Trends in Ecology & Evolution* 33, no. 3: 153–163. https://doi.org/10.1016/j.tree.2017.11.007.

Szymura, J. M., and N. H. Barton. 1986. "Genetic Analysis of a Hybrid Zone Between the Fire-Bellied Toads, *Bombina bombina* and *B. variagata*, Near Cracow in Southern Poland." *Evolution* 40, no. 6: 1141–1159. https://doi.org/10.1111/j.1558-5646.1986.tb05740.x.

Taylor, R. S., and V. L. Friesen. 2017. "The Role of Allochrony in Speciation." *Molecular Ecology* 26, no. 13: 3330–3342. https://doi.org/10.1111/mec.14126.

To, T.-H., M. Jung, S. Lycett, and O. Gascuel. 2016. "Fast Dating Using Least-Squares Criteria and Algorithms." *Systematic Biology* 65, no. 1: 82–97. https://doi.org/10.1093/sysbio/syv068.

Toews, D. P. L., and A. Brelsford. 2012. "The Biogeography of Mitochondrial and Nuclear Discordance in Animals." *Molecular Ecology* 21, no. 16: 3907–3930. https://doi.org/10.1111/j.1365-294X.2012.05664.x.

Tolley, K. A., N. S. Telford, J. M. Taft, et al. 2022. "Taxonomic Inflation due to Inadequate Sampling: Are Girdled Lizards (*Cordylus minor* Species Complex) From the Great Karoo One and the Same?" *Biological Journal of the Linnean Society* 135, no. 1: 1–24. https://doi.org/10.1093/biolinnean/blab119.

Toyama, K. S., P.-A. Crochet, and R. Leblois. 2020. "Sampling Schemes and Drift Can Bias Admixture Proportions Inferred by Structure." *Molecular Ecology Resources* 20, no. 6: 1769–1785. https://doi.org/10.1111/1755-0998.13234.

Wang, J. 2017. "The Computer Program STRUCTURE for Assigning Individuals to Populations: Easy to Use but Easier to Misuse." *Molecular Ecology Resources* 17: 981–990. https://doi.org/10.1111/1755-0998.12650.

Wielstra, B. 2019. "Historical Hybrid Zone Movement: More Pervasive Than Appreciated." *Journal of Biogeography* 46, no. 7: 1300–1305. https://doi.org/10.1111/jbi.13600.

Yaaqoub, A., and A. Essaifi. 2023. "Drainage Rearrangement and Landscape Evolution: Insights From the Moroccan Massif Central." *Geomorphology* 437: 108811. https://doi.org/10.1016/j.geomorph.2023.108811.

Zhang, D., L. Tang, Y. Cheng, et al. 2019. ""Ghost Introgression" as a Cause of Deep Mitochondrial Divergence in a Bird Species Complex." *Molecular Biology and Evolution* 36, no. 11: 2375–2386. https://doi.org/10.1093/molbev/msz170.

Supporting Information

Additional supporting information can be found online in the Supporting Information section. **Table S2:** Results of a multiple regressions on distance matrices analysis estimating the contributions of geographic and ecological distances on genetic differentiation along the two transects. For each transect, the intercept corresponds to the expected F_{st} value when all predictors are null, and β values correspond to the slopes of the regressions on each matrix. The *p*-values were derived from 9999 permutations of the F_{st} matrix. **Table S3:** Time calibration for a selection of nodes with four missing data filtration strategies. Values are expressed in millions of years, with 95% Confidence Intervals given between brackets. **Figure S1:** Impact of m, M, and n parameters on the number of polymorphic loci retained for Assembly 1 (Population genetics analyses). Density plots display the distribution of loci retained per sample for each parameter setting. Asterisks mark total loci retained at an 80% completeness threshold (coloured in red when maximizing the amount of loci retained, a criterion used to select the optimal parameter value). **Figure S2:** Impact of m, M, and n parameters on the number of polymorphic loci retained for Assembly 2 (Phylogeny). Density plots display the distribution of loci retained per sample for each parameter setting. Asterisks mark total loci retained at an 80% completeness threshold (coloured in red when maximizing the amount of loci retained, a criterion used to select the optimal parameter value). **Figure S3:** Plot showing the incremental increase in likelihood (DeltaK) in Structure analyses when increasing the number of genetic groups (*K*) from 2 to 5. The *K* value maximizing DeltaK is considered best-fitting the data. **Figure S4:** Principal Component Analysis within the S-Atl lineage. The top panels show samples plotted on spaces defined by PC1 and PC2 (left) and PC1 and PC3 (right). The variance explained by the PCs is indicated at the axes. The bottom panel shows the sampling map with the different clusters in the PCA highlighted. **Figure S5:** Principal Component Analysis within the Mara lineage. The top panels show samples plotted on spaces defined by PC1 and PC2 (left) and PC1 and PC3 (right). The variance explained by the PCs is indicated at the axes. The bottom panel shows the sampling map with the different clusters in the PCA highlighted. **Figure S6:** Principal Component Analysis within the S-Bou lineage. The groupings do not follow a specific geographic structure. **Figure S7:** Variation of nucleotide diversity along the sampled transects in the three lineages. Red lines show linear regression, and coefficients of determination are indicated. **Figure S8:** Linear regressions between pairwise genetic and geographic distances within the three lineages. The grey areas show confidence intervals around the regression lines, and coefficients of determination are indicated. **Figure S9:** Biplots of a principal component analysis of bioclimatic variables at the sampling localities along the S-Atl to Mara transect. Arrows represent loadings of the 19 bioclimatic variables, scaled with a ×10 factor to improve visualization. **Figure S10:** Biplots of a principal component analysis of bioclimatic variables at the sampling localities along the Atlantic coast transect. Arrows represent loadings of the 19 bioclimatic variables, scaled with a ×10 factor to improve visualization. **Figure S11:** Variation of PC3 score in a principal component analysis of 19 bioclimatic variables along the S-Atl to Mara transect. The vertical black line shows the location of the centre of the cline of genomic ancestries. The red line shows a local regression fitted to the data, with the grey envelope denoting its confidence interval. **Figure S12:** Climatic disparity across localities within and between S-Atl and Mara. Disparity is measured as pairwise distance across localities on the first three axes of a principal component analysis of 19 bioclimatic variables. The significance of right-tailed Wilcoxon rank sum tests is displayed on the right (null hypothesis: between-groups disparity is not higher than within-group disparity). **Figure S13:** Variation of PC3 score in a principal component analysis of 19 bioclimatic variables along the S-Bou to S-Atl transect. The vertical black line shows the location of the centre of the cline of genomic ancestries. The red line shows a local regression fitted to the data, with the grey envelope denoting the confidence interval. **Figure S14:** Climatic disparity across localities within and between S-Bou and S-Atl. Disparity is measured as pairwise distance across localities on the first three axes of a principal component analysis of 19 bioclimatic variables. The significance of right-tailed Wilcoxon rank sum tests is displayed on the right (null hypothesis: between-groups disparity is not higher than within-group disparity). **Table S1:** Samples metadata. List of all samples used in this study with their ENA accession number, associated voucher when available (BEV = 'Biogéographie des Vertébrés' collection in CEFE-CNRS, Montpellier), tissue sample code, dataset

1365294x, 2026, 19, Downloaded from https://onlinelibrary.wiley.com/doi/10.1111/mec.70555 by Uppsala University Library, Wiley Online Library on [20/10/2026]. See the Terms and Conditions (https://onlinelibrary.wiley.com/terms-and-conditions) on Wiley Online Library for rules of use; OA articles are governed by the applicable Creative Commons License

(ingroup or outgroup), lineage allocation based on genetic results, membership coefficient to each lineages as estimated by Structure for $K = 3$ (Q values), country of sampling, locality verbatim, latitude and longitude in decimal degrees (WGS84), accuracy of the coordinates when available (radius of a circle cantered on the coordinates and containing the point of capture), day, month and year of capture, and collectors when available. **Supporting Information: S1.** kml file representing the location of the ingroup samples with the position of the two transects used for the cline analyses.

1365294x, 2026, 19, Downloaded from https://onlinelibrary.wiley.com/doi/10.1111/mec.70555 by Uppsala University Library, Wiley Online Library on [20/10/2026]. See the Terms and Conditions (https://onlinelibrary.wiley.com/terms-and-conditions) on Wiley Online Library for rules of use; OA articles are governed by the applicable Creative Commons License